Relative errors of derived multi-wavelengths intensive aerosol optical properties using CAPS PM$_{SSA}$ SSA, Nephelometer, and TAP measurements

Patrick Weber[1], Andreas. Petzold[1], Oliver F. Bischof[1,2], Benedikt Fischer[1], Marcel Berg[1], Andrew Freedman[3], Timothy B. Onasch[3], Ulrich Bundke[1]

[1]Forschungszentrum Jülich GmbH, Institute of Energy and Climate Research 8 – Troposphere (IEK-8), Jülich, Germany

[2]TSI GmbH, Particle Instruments, Aachen, Germany

[3]Aerodyne Research Inc., Billerica, MA 01821, USA

Correspondence to: Ulrich Bundke (u.bundke@fz-juelich.de)

Abstract. Aerosol intensive optical properties, including like the Ångström exponents for aerosol light extinction, (EAE), scattering (SAE), and absorption, (AAE), or and the single-scattering albedo (SSA), are indicators for aerosol size distributions, chemical composition, and radiative behaviour, and particle contain alsoalso contain source sinformation. The observationDerivation of these parameters requires the measurement of aerosol optical properties at multiple wavelengths, which usually implies involves the use of several instruments. Our study aims to quantify the uncertainties of in the determination of multiple wavelengthsthese intensive properties by using an optical closure approach, using different test aerosols. In our laboratory closure study, we measured the full set of aerosol optical properties for a range of light-absorbing aerosols particles with different properties externally, mixed externally with ammonium sulphate to generate aerosols of with controlled single scattering albedoSSA values. The investigated aerosol absorbing particle types were: fresh combustion soot emitted by an inverted flame soot generator (SOOT, fractal aggregatesagglomerates), Aquadag (AQ, spherical shapecompact aggregates), Cabot industrial soot (BC, compact agglomeratesclusters), and an acrylic paint (Magic Black, MBshape unknown). One focus was on the validity of the Differential Method (DM: absorption = extinction minus scattering) for the determination of Ångström exponents for different particle loads and mixtures of a light absorbing aerosol with ammonium sulphate, in comparison to data obtained from single instruments. The instruments used in this study were two Cavity Attenuated Phase Shift Single Scattering Albedo monitors CAPS PM$_{ssa}$ (CAPS PM$_{SSA}$ Cavity Attenuated Phase Shift Single Scattering Albedo, λ = 450, 630 nm) for measuring light extinction and scattering coefficients, one Integrating Nephelometer (λ = 450, 550, 700 nm) for the light scattering coefficientcoefficients, and one Tricolour Absorption Photometer (TAP, λ = 467, 528, 652 nm) for filter-based light absorption coefficientcoefficients measurement.

Our One key finding is that the coefficients of light absorption σ_{ap}, scattering, σ_{sp} and extinction σ_{ep} derived from combing the measurements of two independent instruments from the Differential Method agree with data measurements from single reference instruments; , and the slopes of regression lines are equal unity within the precision error.reported uncertainties (i.e., closure is observed). Despite closure for measured absorption coefficients, we caution that the estimated uncertainties for absorption coefficients, propagated for the Differential Method (DM: absorption = extinction minus scattering), can exceed 100% for atmospheric relevant SSA values (>0.9). This

increasing estimated uncertainty with increasing SSA yields AAE values that may be too uncertain for measurements in the range of atmospheric aerosol loadings. We recommend using DM for measuring AAE values when the SSA < 0.9. ~~We found, however, that the precision error for the DM exceeds 100% for σ_{ap} values lower than 10-20 Mm^{-1} for atmospheric relevant single scattering albedo. This increasing uncertainty with decreasing σ_{ap} yields an absorption Ångström exponent (AAE) that is too uncertain~~ ambiguous ~~for measurements in the range of atmospheric aerosol loadings. We recommend using DM only for measuring AAE values for σ_{ap} > 50 Mm^{-1}. Ångström exponents for scattering and extinction are reliable~~ EAE and SAE derived values achieved closure during this study within stated uncertainties for extinction coefficients greater than 15 ~~from 20 up to 1000~~ Mm^{-1}. ~~and stay within 10% deviation from reference instruments, regardless of the chosen method. Single scattering albedo (~~SSA~~)~~ values for 450 nm and 630 nm wavelengths internally agreed with each other within ~~values from the reference method σ_{sp} (NEPH)/σ_{ep} (CAPS PM_{SSA}) with less than~~ 10% uncertainty for all instrument combinations and sampled aerosol types which ~~fulfil~~fulfils the defined goals for measurement uncertainty of 10% proposed by Laj et al., 2020 for GCOS (Global Climate Observing System) applications.

1. Introduction

The precise determination of aerosol optical properties is crucial for the provision of reliable input data for chemistry transport models, climate models, and radiative forcing calculations (Myhre et al., 2013). This applies, in particular, to light-absorbing particles like black carbon (Petzold et al., 2013), which are produced by incomplete combustion processes and absorb visible light very efficiently. Aerosol light absorbing properties are also relevant for source appointment studies and the determination of anthropogenic influences on ~~the~~ atmospheric ~~aerosol~~aerosols (Sandradewi et al., 2008)~~.~~ There are two common methods to generate aerosol light absorption ~~data~~ values for long-term and short-term ~~measurements~~monitoring, each with its own disadvantages. One method is a filter-based technique, which operates by deriving light absorbing values from the attenuation of light through particle-loaded ~~filter~~filters (Rosen et al., 1978). A disadvantage of all filter-based methods is linked to ~~effects~~ artifacts like multiple scattering inside the filter matrix, shadowing of light-absorbing particles in highly loaded filters, and humidity effects on the filter substrate (Lack, 2008; Moosmüller et al., 2009). Widely deployed filter-based light absorption ~~measurement methods~~instruments ~~are~~ include the Particle Soot Absorption Photometer (PSAP: Bond et al., 1999~~)~~), ~~and its further development,~~ the Tri-colour Absorption Photometer (TAP), ~~which has a similar design to~~ the ~~CLAP (~~Continuous Light Absorption Photometer~~)~~ ~~(~~(~~TAP~~CL~~TAP~~;~~ ~~(~~Ogren et al., 2017), the Aethalometer (Hansen et al., 1984), and the Multi-Angle Absorption Photometer (MAAP) (Petzold et al., 2005). The PSAP, TAP, CLAP, and ~~TAP~~Aethalometer share their measurement principle, ~~by having~~utilize a reference spot technique, and ~~similar correction schemes. Except for the MAAP, all filter based methods~~ require complex correction algorithms ~~(~~(~~Collaud~~ Coen et al., 2010~~ #285~~; Virkkulaet al., 2010~~ #234~~; Virkkula et al., 2005~~ #95~~)~~). The MAAP utilizes a different approach, a two-stream radiative transport model, made possible by its measurement of both direct transmission and back scatter from the particle loaded filter substrate. Another method for deriving aerosol light absorption ~~coefficients~~ is the differential method, based on the subtraction of light scattering from ~~light~~ extinction ~~coefficients~~. This method

is commonly conducted by comparing measurements from two separate instruments which results in large precision errors particularly for low~~er aerosol~~ light absorption~~ coefficients.~~ and/or high single scattering albedo (SSA) values. In laboratory studies, however, the differential method is widely used as a reference technique because the applied light scattering and extinction instruments make measurements on freely floating particles (i.e., no filter-based artifacts) and are well characterised (Bond et al., 1999; Schnaiter et al., 2005; Sheridan et al., 2005). A significant improvement of aerosol measurement capacities is achieved by the recently developed Cavity Attenuated Phase Shift particle monitor for single scattering albedo (CAPS PM_{SSA}) (Onasch et al., 2015~~b~~), which is able to measure light extinction and scattering simultaneously and is the focus of recent studies (Perim de Faria et al., 2021; Modini et al., 2021)~~.~~.

Intensive aerosol parameters like the Single Scattering Albedo (SSA) or Ångström exponents are often not directly measured, but calculated from multiple instrument datasets, which could lead to an increase in errors and uncertainties ~~concerning this parameter~~. The importance of measuring reliable intensive parameters is undisputable, especially~~,~~ when ~~the use of them~~their use is required for an experiment or sensitive climate related modelling. The Ångström exponents are widely used to adjust extensive parameters to a desired wavelength (Ångström, 1929)~~:~~, ~~Foster et al. (2019)~~ for instrument ~~comparison~~comparisons (Foster et al. 2019), ~~and more importantly~~ for aerosol characterisation (Russell et al., 2010) like the refraction index ~~calculation~~ determination of mineral dust (Petzold et al., 2009) or black carbon (Kim et al., 2015), or for source identification of mineral dust (Formenti et al., 2011). Ångström exponents vary with particle size, shape, and chemical composition, though the relative importance of these factors differ for each optical property. The scattering Ångström exponent (SAE) is most sensitive to particle size ~~size dependent~~ and, therefore, used as an indication of the size distribution of measured aerosols ~~in the investigated medium~~. ~~The~~ A SAE value of 4 indicates either ~~a~~ gaseous Rayleigh scattering or ~~medium or a medium with nanometer~~nanometre-sized particles, whereas a value of 0 indicates coarse particles (Kokhanovsky, 2008). The absorption Ångström exponents (AAE) ~~depends~~is sensitive to ~~on~~ the chemical composition and size of the aerosol particles. A value of 1 indicates an aerosol which absorbs light strongly across the entire visible spectral range and is composed of ~~nanometer~~nanometre-sized ~~spheres~~ spherules (Berry and Percival, 1986). This behaviour is characteristic for fresh soot or black carbon fractal agglomerates (Kirchstetter and Thatcher, 2012; Xu et al., 2015). AAE values higher than unity indicate the presence of brown carbon (Kim et al., 2015) or mineral dust (Formenti et al., 2011), both of which are characterised by a stronger absorption in the blue and ultraviolet compared to the red spectral range. ~~The AAE~~The AAE values > 1 may also occur for coated light absorbing particles (e.g., coated soot) or larger, more compact light absorbing particles ~~could differ when the light absorpbing particle is coated or have a size distribution change {Lack, 2008 ({~~Lack and Cappa, 2010~~) #290} #18}~~. The extinction Ångström exponent (EAE) is often used for aerosol classification by remote sensing methods such as Lidar and depends on particle size ~~distribution~~ and chemical composition (Kaskaoutis et al., 2007; Veselovskii et al., 2016). Combining ~~those~~the~~o~~se Ångström exponents in ~~a~~ cluster ~~plot~~plots is a reliable method for ~~classify~~ classifying aerosol sources (Russell, 2010). The SSA of an aerosol is the key parameter for its direct and semi direct impact on ~~the~~ climate (Penner, 2001). ~~It~~ The SSA describes the ratio of scattering to total extinction of a measured aerosol~~a medium~~. ~~The~~ An SSA value of 1 indicates that light extinction ~~relies~~ occurs exclusively ~~on~~ due to

light scattering. In contrast, ~~low~~ SSA values < 1 indicate an aerosol with a ~~large~~ significant fraction of light-absorbing components, which may cause heating of the atmosphere. The intensive parameters are ~~only~~ commonly available only through multiple-instrument approaches at different wavelengths, which calls for a detailed analysis of their measurement uncertainties. Our study contributes to this topic with a detailed optical closure study, in which we deploy standard and advanced instrumentation for measuring aerosol optical properties and sample mixtures of light absorbing and scattering aerosol to assess method uncertainties and precision errors.

2. Experimental Approach

2.1 Experimental Design

A schematic of the experimental setup is shown in Figure~~.~~ 1. Briefly, aerosol flows, generated using two nebulizers or an inverted flame generator, are dehumidified (generally to below 7%) using ~~silica gel (? Nafion)~~diffusion driers filled with silica gel and sent to a mixing chamber to ensure homogeneous mixing, prior to being sampled using a suite of optical instruments~~ and then onto several measurement instruments~~. In order to avoid particle losses caused by electrostatic forces, all tubing and chambers are constructed of either stainless steel or conductive silicone tubing. The individual optical instruments are connected using an iso-axial orientated and isokinetic operated nozzle located in the centreline of the supply line. As shown ~~above~~in Figure 1, aerosol~~The aerosol~~ production was controlled by multiple Mass Flow Controllers (MFC, Bronkhorst High-Tech B.V., Ruurlo, Netherlands). A Labview based program~~me~~ controlled the complete measurement system and ~~recorded~~ centrally recorded all data from the individual instruments. ~~Downstream of the aerosol production, the aerosol was injected in a mixing chamber assuring homogenous mixing~~ ~~Downstream the production the aerosol was injected in a mixing chamber assuring homogenous mixing~~. ~~The mixing chamber is attached to the aerosol supply line.~~ ~~Several instruments are connected to the central aerosol supply line.~~ Pressures in the aerosol delivery lines were maintained at that of the ambient atmosphere at all times. Aerosol flow rates to the individual instruments were provided at their specified levels (0.~~5~~6 - 3.0 lpm) except for that of the TSI nephelometer. Given the limitations of the aerosol supply system, the flow to the nephelometer was reduced from 20 lpm to ~2.2 lpm, causing the physical response time of that instrument to be increased to ten minutes. Complete details of the generation of aerosols ~~is~~are provided in the following section.

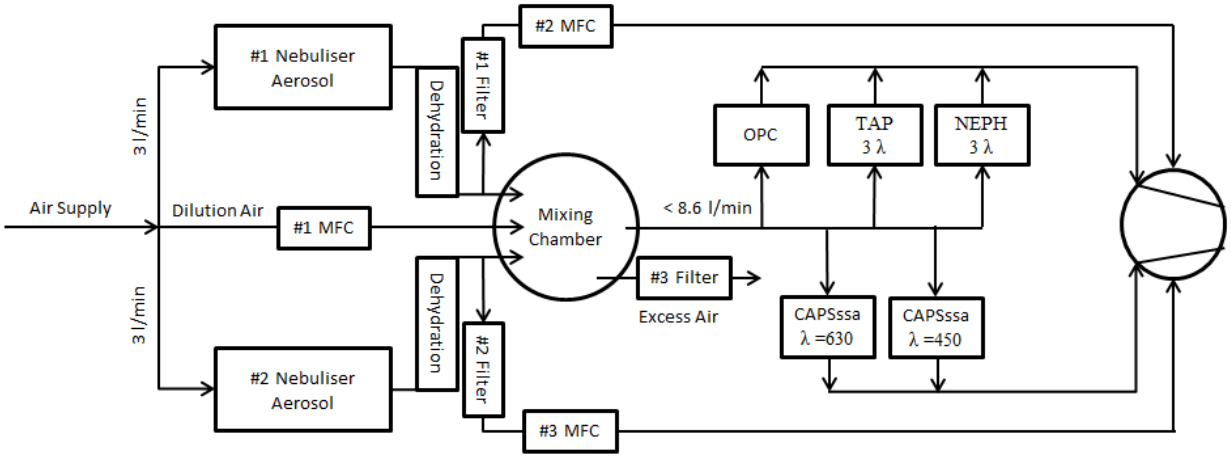

Figure 1. Experimental setup for the ~~initial~~ measurements. ~~Additional~~Flame soot measurements were done with a combustion flame source replacing #2 Nebuliser.

The generated aerosol size distributions were characterized and monitored with either a Scanning Mobility Particle Sizer (SMPS) composed of the combination of a Differential Mobility Analyzer (DMA 5.400, Grimm Aerosol Technik GmbH Co & KG Germany) and Condensation Particle Counter (CPC 5.411, Grimm Aerosol Technik) system in a sequential mode of operation or a~~A~~ Grimm optical particle size spectrometer (SKY-OPC, model 1.129, Grimm Aerosol GmbH & Co. KG, Ainring, Germany) ~~was used to characterize and monitor the resulting size distribution~~.

2.2 Optical Instruments and Uncertainties

~~where t~~The individual instruments are connected ~~to using an iso-axial orientated and isokinetic operated nozzle located in the centreline of the supply line.~~ The suite of optical instruments used in this study included the following instruments. ~~A Grimm optical particle size spectrometer (SKY-OPC, model 1.129, Grimm Aerosol GmbH & Co. KG, Ainring, Germany) was used to characterize and monitor the resulting size distribution.~~ The particle scattering coefficient, σ_{sp}, was measured with a~~n~~ integrating multi wavelength nephelometer (NEPH, Model 3563, TSI Inc., Shoreview, MN, USA; ~~)~~ ~~(~~Bodhaine et al., 1991) and ~~by~~ with the scattering channel ~~an integrating sphere used in~~of the CAPS PM_{SSA} monitor (CAPS PM_{SSA}, Aerodyne Research Inc., Billerica, MA, USA; Onasch et al. (2015~~)).~~), which is derived from a measurement of the total extinction and single scattering albedo. For the particle light absorption coefficient, σ_{ap}, we used the ~~small sized~~ Tricolor Absorption Photometer (TAP (Brechtel Inc., Hayward, CA, USA), which is based on the well-known Particle Soot Absorption ~~Particle Soot Absorption~~ Photometer (PSAP, ~~(~~ARM Research) and the Continuous Light Absorption Photometer (CLAP) developed by NOAA (Ogren et al., 2017). The particle light extinction coefficient, σ_{ep}, was directly measured with the phase shift channel of the CAPS PM_{SSA} monitor.

The light extinction channel of the CAPS instrument has an uncertainty of 5% and a precision of 2% and a scattering uncertainty of 8% and 2% precision, respectively (Onasch et al., 2015). The TAP has an uncertainty of around 8%, with a precision of 4% ((Müller et al., 2014; Ogren et al., 2017), while the NEPH has an uncertainty of less than 10%

and a precision of about 3% (Anderson and Ogren, 1998 Massoli et al., 2009). These literature-derived uncertainty estimates for measurement accuracy will be used in this study for instrument closure, either directly or via error propagation. Individual point averages will be shown with corresponding precision variances.

2.32 Aerosol Generation

Table 12 provides a complete list of all aerosol ~~species~~types used in the ~~measurements~~study. Solutions of known concentrations of Aquadag (AQ, Aqueous Deflocculated Acheson Graphite; Acheson Industries, Inc., Port Huron, MI, USA), Cabot Black (BC) ~~or~~and ~~the Acrylic Paint~~ Magic Black (MB), an acrylic based paint, were prepared on a daily basis by ultra-sonication before nebulization in a Constant Output Atomizer (Model 3076, TSI Inc.). The count median diameter (CMD) and geometric standard deviation (GSD) of the ammonium sulphate nebulized by the constant output atomizer depends on the concentration of the salt solution and the flow~~s~~ through the atomizer ~~is operated with~~. Use of constant -flow rates and particle concentrations ~~also~~ produced~~s~~ constant size distributions (Liu et al. 1975). The inverted flame soot generator (Argonaut Scientific Corporation, Edmonton, AB, Canada) was operated with a pre-determined propane to oxidation air ratio of 7.5 litre per minute air to 0.0625 litre per minute propane so that the flame produced a stable and low organic carbon soot. It has previously been shown that at least 30 min were necessary for the Argonaut flame to reach stable aerosol concentrations (Bischof et al., 2019; Kazemimanesh et al., 2018).

Initially, pure aerosol types were generated independently and measured to quantify their size distributions and optical properties. The main part of the study was focused on making external mixtures of ammonium sulphate and each of the absorbing particle types, separately. These mixtures were controlled to provide a stable aerosol with varying intensive optical properties.

~~With these sets of different aerosol types and shapes, the behaviour of instrument measurement is investigated. The results of the intercomparison of Aquadag is expected to be best described by Mie theory, since it has a near spherical~~ ~~spherically shape. and thereforeTherefore, applied correctionthe correction schemes applied to the instruments apply best, since calibration is done by ideal PSL spheres (polystyrene latex beads), which were treated the same as all other aerosol solution samples and their size was approved confirmed by DMA and OPC measurements . Fractal agglomerates could have multiple internal scattering effects. Spherical shapes and several optical properties are determined by determined of the primary particle, this is expected to differ the most in intercomparison approaches (Barber and Wang, 1978; Moosmüller et al., 2009).~~

Table 21. Overview of aerosol types used.

Substance	Aerosol type	Acronym	Shape
Ammonium Sulphate	salt	AS	spheroidal
Aquadag	colloidal graphite	AQ	compact aggregates
Cabot Black (Regal 400R)	powder	BC	compact agglomerates

Flame Soot	combustion aerosol	Soot	fractal agglomerates
Magic Black (Acrylic paint)	organic pigments	MB	~~spheroidal (?)~~unknown

2.~~4~~3~~2~~. ~~2~~ Data ~~analysis~~Treatment

2.~~2~~.2.~~43~~.1 Instrument ~~1~~ Corrections and C~~c~~alibrations

The CAPS PM_{SSA} instrument extinction channel was calibrated ~~with~~ using polystyrene latex beads (PSL) particles as a reference standard and Mie theory using ~~the~~a BHMIE Python code derived from Bohren & Hoffman (1983). Additionally, the 450 nm wavelength CAPS PM_{SSA} calibration was validated using ~~was calibrated with~~measurements of CO_2 Rayleigh scattering ~~for additionally calibrated with CO_2 for further validation of the same geometric factor for the CAPS sampling cells. validating the same factor and The NEPH was calibrated using CO_2 the calibration was applied to the nephelometer (Anderson and Ogren, 1998; Modini et al., 2021).~~ The scattering channel of the CAPS PM_{SSA} ~~using the integrating sphere method~~ was internally adjusted to the extinction channel using ammonium sulphate as a light-scattering aerosol, assuming a single scattering albedo of 1.0.~~,~~ A truncation error correction was not necessary regarding the size of the aerosols used (Onasch et al., 2015~~a~~), since ~~the highest amount of aerosols were was~~all the aerosols used had median diameter smaller than 200 nm ~~in diameter size, as well that the ammonium sulphate truncation correction is already done by the SSA adjustment~~. The CAPS PM_{SSA} monitor, which ~~has a drifting shift of the base line~~ is subject to baseline drift as the ~~as long as the~~ system ~~is heating~~heats up, ~~which apparently~~ stabilized after 30 min of operation (Faria et al., 2019). ~~This was considered during the experiment, means that the instruments had a long HEPA Filter induced warm up period, were no data was taken.~~.

The NEPH was calibrated using CO_2 (Anderson and Ogren, 1998; Modini et al., 2021). Truncation corrections were made using the approaches developed by Anderson and Ogren (1998) for purely scattering aerosols ~~The nephelometer (NEPH)~~and by Massoli~~,~~ et al. (2009) for aerosol mixtures containing light absorbing particles ~~correction for light absorbing aerosols was calculated according to~~ (Massoli et al., 2009). ~~In any case, t~~The truncation corrections applied were always equal to or less than 5%. ~~.~~Because of the reduced air flow, the ~~nephelometer~~ NEPH needed at least 15 minutes to reach a stable plateau after changing aerosol ~~production~~ generation settings.

~~After that, a~~A new f~~F~~ilter s~~S~~pot for the TAP was selected~~,~~ for each measurement in order to minimize measurements ~~transmission~~ uncertainties ~~increases by~~due to particle loaded filters. The first correction regarding truncation is done by the included Software. The software has the capability to choose the ~~correct~~ Ogren correction scheme based on the filter type used (Quartz Fibre, BT-TAP-FIL100, ENVILYSE). Further corrections were made according to Virkkula, (2010). ~~not sure exactly what gives here. Does the monitor software perform any corrections?~~

Table ~~1~~2. List of applied correction algorithms to optical instruments.

Instrument	Manufacturer	Properties	λ (nm)	Reference
CAPS PM_{SSA}	Aerodyne Research Inc.	σ_{ep}; σ_{sp}	450; 630	Onasch et al. (2015)

NEPH	TSI Inc.	σ_{sp}	450; 550;700	Anderson and Ogren (1998)–; Massoli et al. (2009)
TAP	Brechtel Inc.	σ_{ap}	467; 530; 660	Virkkula ——(2010); Virkkula (2005)

2.2~~2.4~~3.2 Aerosol Optical ~~Probertites~~ Properties derived from primary measurements

The extensive parameters for aerosol light interactions are extinction, scattering and absorption. When two of them are known, the missing one can be calculated with the help of this equation:

$$\sigma_{ep} = \sigma_{sp} + \sigma_{ap} \quad \text{Eq. (1)}$$

where σ_{ep} is the extinction coefficient, σ_{sp} the light scattering coefficient and σ_{ap} the coefficient for light absorption by particles. The unit of all these parameters is Mm^{-1} ("inverse Mega meters"; 1 $Mm^{-1} = 10^{-6}\ m^{-1}$). When ~~S~~solving equation 1 for σ_{ap}, it is possible to derive the absorption coefficient by combining CAPS PM_{SSA} extinction measurements ~~CAPS_SSA and~~with either CAPS PM_{SSA} or ~~nephelometer~~ NEPH scattering measurements [σ_{ap}(CAPS, CAPS) or σ_{ap}(CAPS, NEPH)] for comparison. In the following, this will be called the Differential Method (DM).

To calculate the Single Scattering Albedo (SSA), the particle light scattering must be divided by the particle light extinction:

$$(\lambda) = \frac{\sigma_{sp}}{\sigma_{ep}} \quad \text{Eq. (2)}$$

The Ångström exponents (AE) are calculated from:

$$xAE = -\frac{\log\left(\frac{\sigma_{xp}(\lambda 1)}{\sigma_{xp}(\lambda 2)}\right)}{\log\left(\lambda 1/\lambda 2\right)} \quad \text{Eq. (3)}$$

By solving Eq. 3 for $\sigma_p(\lambda 1)$ and assuming a valid Ångström exponent the resulting equation (3a) is used for wavelength adjustments

$$\sigma_{xp}(\lambda 1) = \sigma_{xp}(\lambda 2) \cdot \left(\frac{\lambda 1}{\lambda 2}\right)^{-AE} \quad \text{Eq. (3a)}$$

For the particle coefficient σ_{xp}, the corresponding σ_{sp}, σ_{ep}, or σ_{ap} could be put into calculations (Eq. 3) to obtain the absorption Ångström exponent (AAE), extinction Ångström exponent (EAE) and scattering Ångström exponent (SAE), accordingly.

2.~~4~~3.~~2~~3~~2.2.3~~ Error propagation

Error propagation ~~for precision errors Δ~~ are determined by Gaussian error propagation:

$$SSA(\lambda, \sigma_{sp}, \sigma_{ep}) = \frac{\sigma_{sp}}{\sigma_{ep}} \quad \xrightarrow{yields} \quad \Delta\text{SSA}\ (\lambda, \sigma_{sp}, \sigma_{ep}) = \sqrt{\left(\frac{1}{\sigma_{ep}} \cdot \Delta\sigma_{sp}\right)^2 + \left(\frac{\sigma_{sp}}{\sigma_{ep}^2}\Delta\sigma_{ep}\right)^2} \quad \text{Eq. (4)}$$

$$SSA(\lambda, \sigma_{sp}, \sigma_{ap}) = \frac{\sigma_{sp}}{\sigma_{ap+\sigma sp}} \xrightarrow{yields} \Delta\text{SSA}\ (\lambda, \sigma_{sp}\sigma_{ap}) = \sqrt{(\frac{\sigma_{sp}}{(\sigma_{ap+\sigma_{sp}})^2} \cdot \Delta\sigma_{sp})^2 + (\frac{\sigma_{ap}}{(\sigma_{ap+\sigma_{sp}})^2} \cdot \Delta\sigma_{ap})^2} \quad \text{Eq. (5)}$$

$$AE = -\frac{\log(\frac{\sigma_{xp}(\lambda 1)}{\sigma_{xp}(\lambda 2)})}{\log(\lambda 1/\lambda 2)} \xrightarrow{yields} \Delta AE = \sqrt{(\frac{-1}{\log(\lambda 1/\lambda 2)\cdot\sigma_p(\lambda 1)} \cdot \Delta\sigma_{xp}(\lambda 1))^2 + (\frac{1}{\log(\lambda 1/\lambda 2)\cdot\sigma_{xp}(\lambda 2)} \cdot \Delta\sigma_p(\lambda 2))^2} \quad \text{Eq (6)}$$

where $\sigma_{xp} = \{\sigma_{ep}, \sigma_{sp,}\sigma_{ap}\}$

Those equations could be expanded, if the instruments where not calibrated properly, as Sherman (2015) proposed, but are in accordance with the BIPM (Bureau International des Poids et Mesures)

2.4.4 Data Averaging

For each experiment run, a different aerosol mixture was generated with different optical properties and allowed to reach steady state, including waiting ~15 minutes due to the slow time response of the low flow NEPH. At steady state conditions, we measured size and optical properties fluctuating <2% over time with the OPC, CAPS PM_{SSA}, and NEPH. All instruments recorded data at a 1 second rate. Reported data points are given as averages of 100 seconds of stable aerosol production. This value was chosen to obtain a minimum in data precision and detection limits as determined from Allan Standard Deviation plots by Massoli et al. (2010) for the CAPS extinction measurements and Ogren et al. (2017) for filter-based absorption measurements. Averaging for longer periods would only increase variances due to transmission (TAP) and baseline drift (CAPS).

3. Measurements

3.1 Pure aerosol types

The measured size parameters and calculated intensive parameters of the pure aerosol types are summarized in Table 3. The errors reported in Table 3 are calculated from ~~measurement precision~~ error propagation. The size distributions of the different aerosol types were measured with a Grimm SMPS and are shown in Figure 2~~Figure 2~~ normalized to 1000 particles per cubic centimetre. The Ångström exponents for the pure substances ~~are~~fall within typical ranges for these types of aerosols and size distributions reported in literature. For example, the SAE decreases from a value of 3.22 for 40 nm AS particles which is close to the SAE value of 4 for air molecules with increasing particle diameter. Thus, the SAE drops to 0.76 for 130 nm compact AQ particles but increases to 0.99 ~~again~~ for 140 nm fractal agglomerate Soot. ~~-~~The shape of AQ is assumed to be more compact than the soot agglomerates, such that their scattering and electrical mobility behaviours are dependent mainly upon their physical diameters. In contrast, the scattering behaviour of the fractal soot agglomerates is due mainly to the distribution of primary particles, whereas their electrical mobility diameter is more dependent upon the major axis of the agglomerate. As expected by Eq. 3a, the SSA increases with ~~shorter~~decreasing wavelength (Bohren and Huffman, 1983). The AAE for fractal combustion soot is close to 1 as reported by ~~e.g. (~~Török (~~,~~2018) for the mini-CAST soot generator.

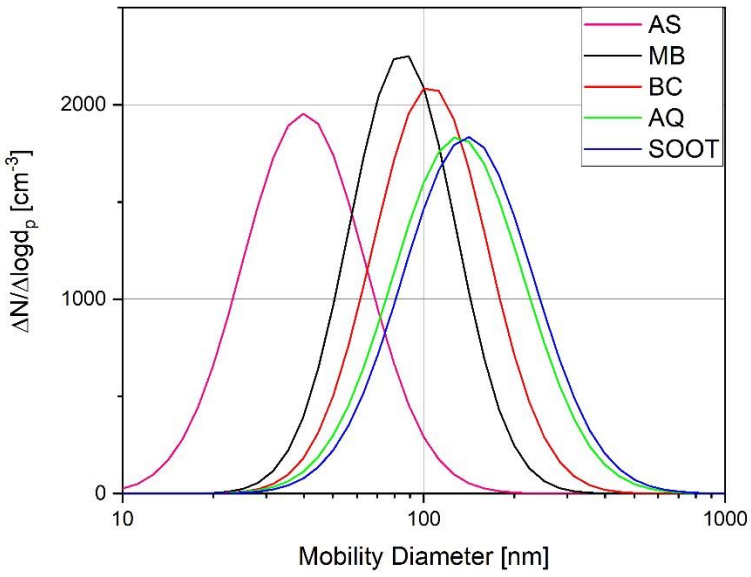

Figure 2. Measured ~~s~~Size ~~D~~distributions by ~~DMA and CPC~~SMPS for the pure aerosol types used, normalised to an assumed total concentration.

~~The errors reported are either the instrument's uncertainties or are calculated from error propagation. The light extinction channel of the CAPS instrument has an uncertainty of 5% and a precision of 2% and a scattering uncertainty of 8% and 2% precision respectively (Onasch et al., 2015). The TAP has an uncertainty of around 8%, with a precision of 4% ((Müller et al., 2014; Ogren et al., 2017), while the nephelometer has an uncertainty of less than 10% and a precision of about 3% (Anderson and Ogren, 1998 Massoli et al., 2009).~~

Table 3. Overview of the measured intensive optical properties of the pure aerosol types.

	AS	**MB**	**BC**	**AQ**	**Soot**
Count Median Diam.	40 nm	85 nm	105 nm	130 nm	140 nm
Geometric Standard Deviation	1.60	1.50	1.55	1.65	1.65
SSA 630 (NEPH, CAPS)	1.0	0.85 ± 0.02	0.26 ± 0.03	0.37 ± 0.03	0.20 ± 0.02
SSA 450 (NEPH, CAPS)	1.0	0.92 ± 0.07	0.32 ± 0.04	0.44 ± 0.02	0.26 ± 0.08
SAE (630/450) (NEPH)	3.22 ± 0.09	2.16 ± 0.37	1.71 ± 0.13	0.76 ± 0.06	0.99 ± 0.08

AAE (630/450) (TAP)	-	1.34 ± 0.12	1.16 ± 0.03	0.44 ± 0.02	1.08 ± 0.02
EAE (630/450) (CAPS)	3.21 ± 0.08	2.03 ± 0.38	1.43 ± 0.65	0.52 ± 0.10	1.10 ± 0.10

3.2~~1~~ Extensive Parameters of Aerosol Mixtures

~~In a first step~~First, the extensive parameters must be validated for all instrument combinations to ensure the reliability of the intensive parameters derived from them. We have chosen to use external mixtures of AS and AQ particles for these studies as they are both readily atomized, generating highly stable aerosols for the necessary time periods for averaging. We note that AQ absorbing aerosols are ~~Aquadag is well-known for its physical properties and it is easy to handle by nebulising. We have selected AQ as it is~~ commonly used as a reference material for instrument comparisons (Foster et al., 2019)~~ for all the viewgraphs~~. The results for mixtures of AS with the other absorbing aerosol types are ~~added~~ included in ~~the associated t~~Tables 6-9. ~~Respective data points are given as averages of at least 100 seconds of stable aerosol production. All instruments recorded data at a 1 second rate. We kept the aerosol in the line in a steady state, which had a fluctuation measured with the OPC, CAPS PMssa and NEPH below 2% deviation. We decided to average these 1Hz data for all instruments for intercomparison within the 100sec after the nephelometer becomes stable.~~

The two CAPS PM_{SSA}~~CAPS SSA~~ monitors (450 nm and 630 nm wavelengths) ~~used~~ measured the extinction coefficient of particles directly with a small precision error of around 2% (Modini et al., 2021)~~ for 450 nm and 630 nm wavelengths~~. In Figure 3~~Figure 3~~Figure 3, we show scatter plots of these direct extinction coefficient measurements (X-axis) in comparison to the ~~combined measurements of the (~~absorption coefficient measured~~)~~ using TAP and the scattering coefficient measured using ~~the nephelometer~~ NEPH combined using Equation (Eq. 1) in the form: $\sigma_{ep}(NEPH, TAP) = \sigma_{ap}(TAP) + \sigma_{sp}(NEPH)$ (y-axis) for wavelengths of 450 nm (right panel) and 630 nm ~~wavelength~~ (left panel).

Formatte

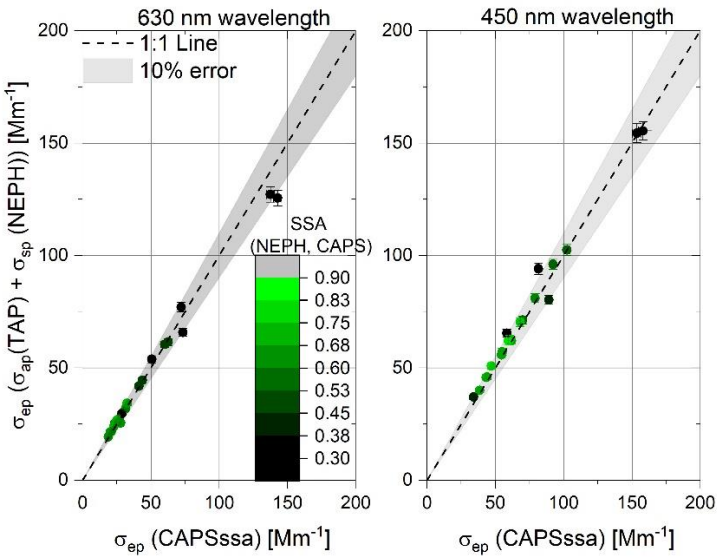

350

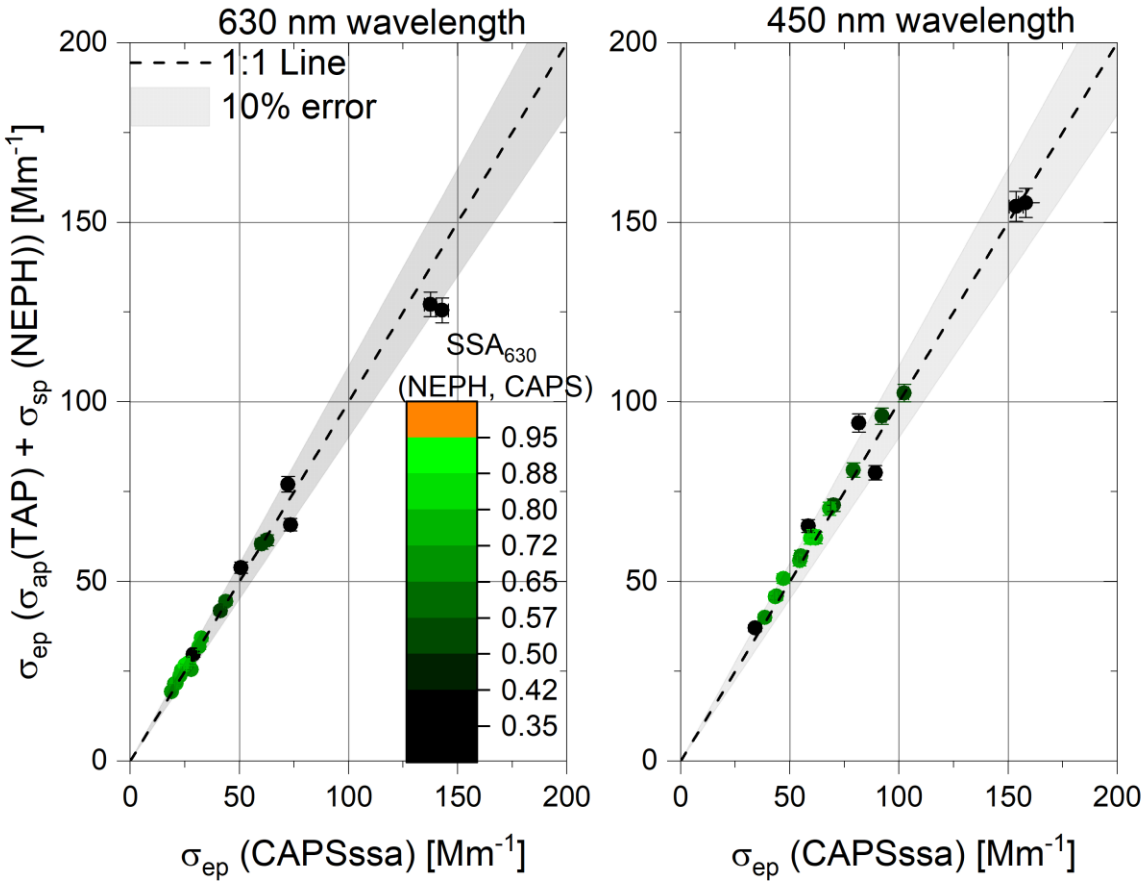

Figure 3. Scatter plots of the ~~e~~Extinction coefficients for different ~~Aquadag~~AQ ~~-~~-AS external mixtures ~~for~~ at 630 nm (left) and 450 nm wavelengths (right). The y-axes show the extinction coefficients ~~measured~~ derived by ~~the~~ combin~~inged~~ TAP absorption and ~~Nephelometer~~ NEPH scattering ~~data of absorption and scattering~~ coefficients versus

the CAPS PM_{SSA} ~~CAPS_SSA~~ monitor direct extinction coefficient measurements. The colour code represents the SSA of the analysed mixed aerosol measured ~~of the respective data point~~ at 630 nm wavelength. In addition, an error band of ±10% was added to the 1:1 line.

Here, the measured 630 nm SSA colour code serves as a proxy for the mixing ratio of the external mixtures of nebulized ~~Aquadag~~ AQ ~~particles~~ and ~~ammonium sulphate~~AS particles ~~are used as a proxy for the mixing ratio the SSA is shown as colour code~~. The measured 630 nm and 450 nm extinction coefficients align with the 1:1 line within 10% ~~in~~ across a broad range ~~of the extinction coefficient for~~of extinction ~~450 and 630 nm wavelength~~ values as well as ~~for~~ SSA values, ~~of the mixtures~~ ranging from 0.3 to close to 1. The 10% was chosen to show the fulfilment of the requirements of ~~{~~Laj, 2020 ~~#293}~~for aerosol properties. This shows that the instruments are not sensitive to the SSA of the particle type used ~~for~~ at ~~both~~ either wavelength~~s~~ of interest.

~~As the next extensive parameter, t~~The measured scattering coefficients at 450 and 630 nm wavelengths are compared using scatterplots for the different techniques in Figure 4~~Figure 4~~Figure 4. Here, we use the ~~Nephelometer~~ NEPH and the integrating sphere channel of the CAPS PM_{SSA} ~~CAPS_SSA~~ instrument capable of measuring the scattering coefficient directly. In addition, we calculated the scattering coefficients using a Differential Method (DM), solving Eq.(1) for the scattering coefficient by subtracting the absorption coefficient measured by the TAP from the extinction coefficient measured by CAPS PM_{SSA} ~~CAPS_SSA~~, The ~~nephelometer~~ NEPH is used as reference because it has well proven correction functions for light absorption particles, as described in Section 2.~~4~~2.1.

Formatte

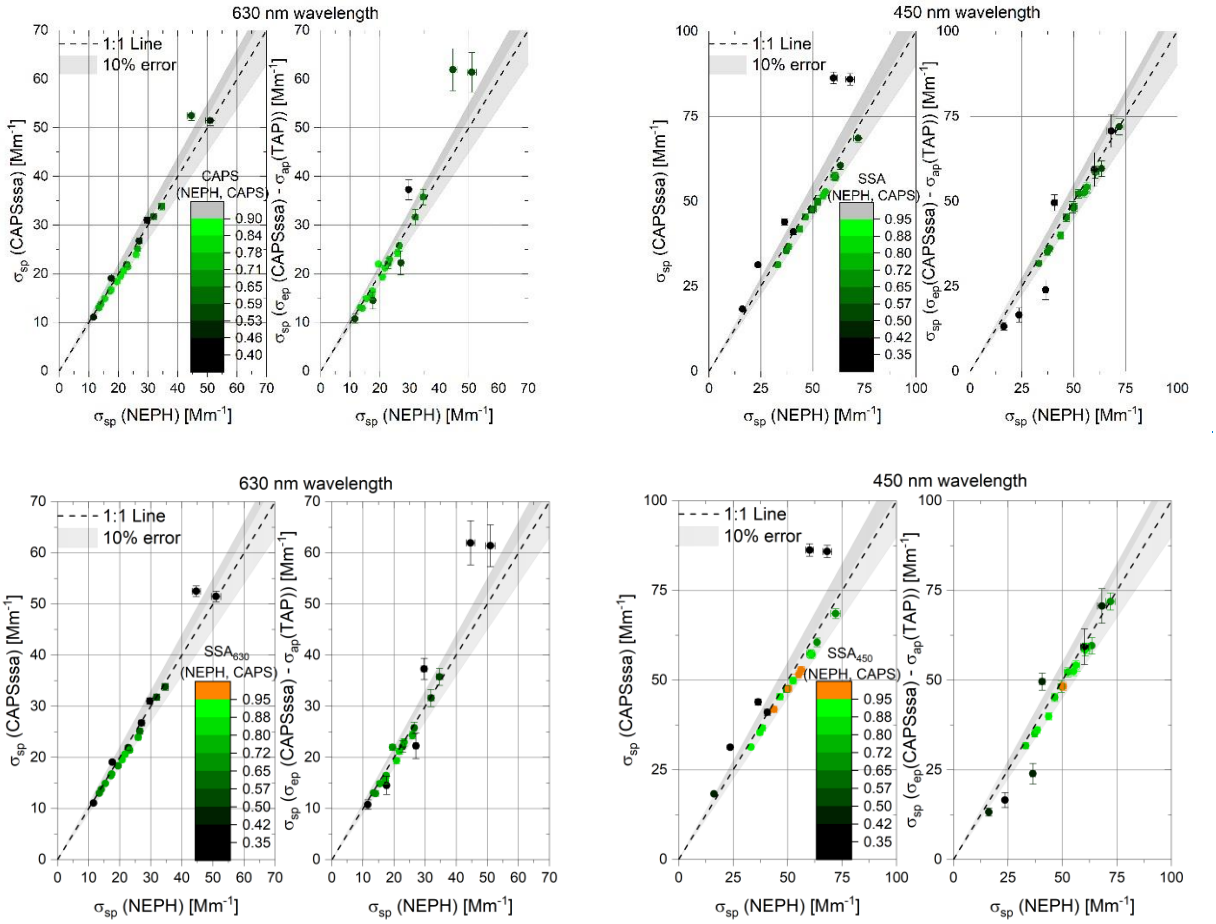

395 **Figure 4.** Comparisons of measured l~~L~~ight scattering coefficients at 450 nm and 630 nm wavelengths for~~of~~ mixtures of ~~Aquadag~~ AQ ~~with~~ and AS aerosols. The y-axes show ~~for 450nm and 630 nm wavelengths for Differential method (DM),~~ the CAPS PM_{SSA} ~~CAPS_SSA~~ (integrating sphere) or the Differential Method (CAPS extinction minus TAP absorption) scattering ~~techniques~~ versus ~~nephelometer~~ NEPH scattering measurements ~~for~~ at 450 nm and 630 nm wavelength~~s using scatter plots~~. The colour code represents the SSA value of the measured aerosol mixture. An error
400 band of ±10% was applied to the 1:1 line. Error bars shown represent ~~one sigma of~~ instrument precisions (1 σ).

The measured scattering coefficients at both 450 nm and 630 nm wavelengths agree~~s~~ within 10% for the majority of measurements~~between the reference instrument in comparison to the internal scattering signal measured with the CAPS PM_{SSA} and σ_{sp} obtained by subtraction of σ_{ap}(TAP) from σ_{ep}(CAPS) shown in Figure 4 within 10% margin.~~ .
405 There is ~~neither~~no apparent ~~a~~ dependence of measured scattering coefficients with scattering coefficient magnitude (over the range measured) nor with aerosol SSA, an indicator of the external mixing ratio~~the mixture ratio with ammonium sulphate (which the SSA is the indicator) visible, nor a dependency as function of light absorbing aerosol loadings~~ ~~There is neither a trend visible of the mixture ratio with ammonium sulphate, which the SSA is the indicator for, nor a strong shift for high or low volumetric cross section values~~. ~~This is true for both examined wavelengths of~~
410 ~~630 nm and 450 nm.~~ Several outliers are visible, particularly for points with SSA values ~ 0.35, indicating nearly pure

AQ aerosols. For the scattering coefficients derived using the Differential Method (CAPS extinction minus TAP absorption), some of the scatter may be due to the larger uncertainties associated with the filter-based absorption measurements, as discussed in the Reno Study (Sheridan, 2005). The outliers in the CAPS vs NEPH plots, especially at 450 nm wavelength, are currently unexplained and are likely due to apparent stability issues for these points. ~~Overall, it is visible, that some data points scatter more roughly on the 1:1 line, which is true for mostly pure Aquadag aerosols, where the TAP contributes the biggest uncertainties due to higher values and deviates from high agreement, which was approved by the Reno Study (Sheridan, 2005) and although visible in our measurements. When the 1σ precision errors are tripled, it is still undistinguishable from the 1:1 line. (Neph truncation~~

Particle light absorption coefficient measurements are the most complicated, as none of our optical instrument techniques directly measure absorption. We have two methods for measuring absorption coefficients: (1) Differential Method following Eq.(1), using either $\sigma_{ap}(CAPS,NEPH) = \sigma_{ep}(CAPS) - \sigma_{sp}(NEPH)$ or $\sigma_{ap}(CAPS,CAPS) = \sigma_{ep}(CAPS) - \sigma_{sp}(CAPS)$; and (2) filter-based TAP measurements. As the~~As a last extensive parameter, we focused on the particle light absorption coefficient. This is the most complicated to measure, as for~~ filter-based method~~s a bunch quantity of~~requires the application of multiple, empirical correction schemes, we have chosen $\sigma_{ap}(CAPS,NEPH)$ as the reference for the comparison of the $\sigma_{ap}(TAP)$ and $\sigma_{ap}(CAPS,CAPS)$ values. ~~must be applied. Using a differential method e.g. ($\sigma_{ap}(CAPS,NEPH) = \sigma_{ep}(CAPS) - \sigma_{sp}(NEPH)$ following Eq.. 1) is used, we have to deal with large relative errors. Because of the availability of reference and calibration substances for filter based methods, $\sigma_{ap}(CAPS,NEPH)$ is given as the reference for the comparison to the $\sigma_{ap}(TAP)$ values and the internal $\sigma_{ap}(CAPS,CAPS)$.~~

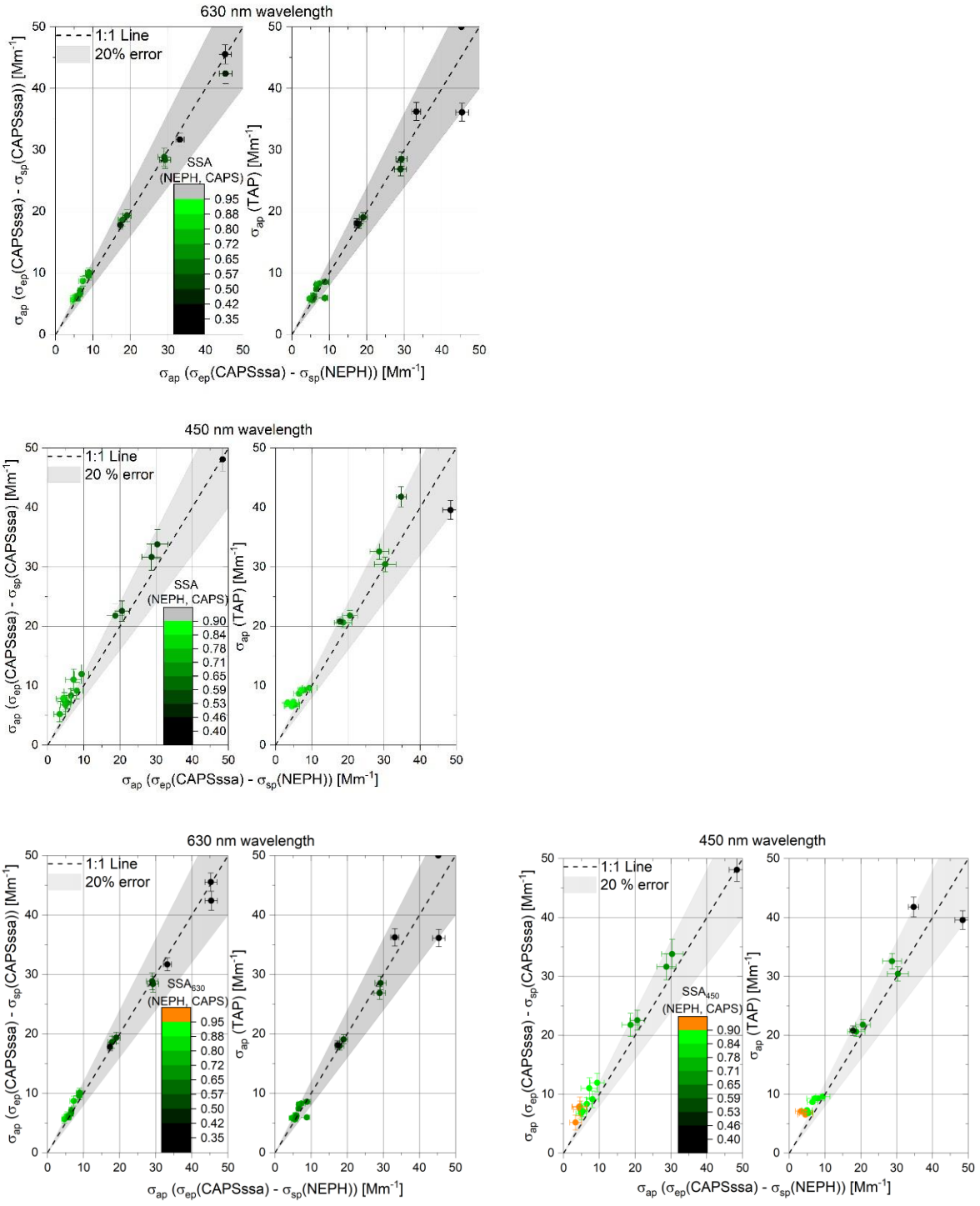

Figure 5. Scatter plots of measured 450 nm and 630 nm wavelength absorption coefficients of external mixtures of ~~Aquadag~~ AQ and AS ~~for 450 nm and 630 nm wavelengths~~ for different instrument combinations. The colour code represents the SSA value of the respective data point. An error band of ±20% was applied to the 1:1 line, which is required by Laj (2020) for light absorption ~~,~~measurements. Error bars shown represent propagated instrument precisions (1 σ). ~~Individual error bars represent variances during on type of mixture produced.~~

In Figure 5~~Figure 5~~Figure 5, the light absorption ~~values~~ measurements ~~for~~ at wavelengths of 450 nm and 630 nm are ~~depicted~~compared. We chose to include 20% error bands for these comparisons, though ~~To compare instruments,~~ the overall uncertainty for filter-based absorption measurements is often estimated to be 30% (Bond et al., 1999). ~~In this work we stay within a 20% deviation for this parameter.~~ Most of the data points shown fall within the 20% error band, with some exceptions for aerosols with low absorption and high SSA values. ~~correlated for both the σ_{ap}(CAPS,CAPS) and σ_{ap}(TAP) reference, without any mixing ratio dependence. When the σ_{ap}(CAPS,CAPS)is compared to σ_{ap}(CAPS,NEPH), the values agree within the uncertainty errors.~~

Table ~~4~~4. Linear regression ~~analysis~~ results of ~~attenuation~~ scattering, σ_{sp} , extinction, σ_{ep}, and absorption, σ_{ap}, coefficients from Figures 3-5 for ~~of~~ external mixtures of AQ and AS particles,~~Aquadag and ammonium sulphate mixtures~~ given as slopes (m), Pearson R, and y-axis ~~intersection~~ intercepts (b).

	σ_{sp} (CAPS) vs. σ_{sp} (NEPH)	$\sigma_{sp(CAPS,TAP)}$ vs. $\sigma_{sp(NEPH))}$	$\sigma_{ep(NEPH,TAP)}$ vs. $\sigma_{ep(CAPS)}$	$\sigma_{ap(TAP)}$ vs. $\sigma_{ap(CAPS,NEPH)}$
		630 nm		
m	1.07 ± 0.03	1.08 ± 0.05	0.99 ± 0.03	0.92 ± 0.07
R	0.99	0.97	0.99	0.95
b [Mm^{-1}]	-1.84 ± 0.57	-2.15 ± 1.12	0.91 ± 0.93	0.78 ± 0.68
		450 nm		
m	0.99 ± 0.05	1.06 ± 0.03	0.98 ± 0.03	1.04 ± 0.08
R	0.97	0.99	0.99	0.96
b [Mm^{-1}]	1.14 ± 2.27	-4.60 ± 1.51	3.37 ± 1.71	2.13 ± 0.64

The high Pearson correlation (~~r~~R > 0.95) coefficients in ~~Table 4~~Table 4 indicate that the correlations ~~is~~ are highly linear ~~and reveals a stable behaviour of the instrument measurements characteristics~~. ~~The light extinction reached over 850 Mm^{-1} and light absorption over 200 Mm^{-1} for 450 nm wavelengths with values starting from 3 Mm^{-1} for light absorption for 450 nm wavelength.~~ The ~~primally~~primary focus for this study was to have ~~the~~ most of the experimental runs exhibit light extinctions between 5 Mm^{-1} ~~and~~ and 1500 Mm^{-1}, representative of atmospheric conditions ~~for light extinction~~. ~~The~~ The slopes are all close to unity within the expected errors ranges, or at least single instrument uncertainty, indicating closure has been achieved for these optical measurements. Thus, the extensive parameters can be trusted for instrument comparison, especially for the light scattering and light extinction information. ~~The slopes reported for light absorption coefficients are with 0.,92 ±0.07 and 1.04 ±0.08 below the expected error from literature. Higher values influence linear regression slopes, for which the filter methods are drifting to lower values respective to~~

~~intercomparison instruments (Sheridan, 2005).~~ We provide ~~further~~ regression analys~~e~~is for all other absorbing aerosol types ~~individually~~ externally mixed with AS in Tables 7-9.

~~An e~~Excellent agreement (R~~²~~>~~=~~0.9~~79~~) is shown for σ_{sp} measurements of the ~~nephelometer~~ NEPH and the CAPS PM_{SSA} scattering channel, ~~. Thus,~~indicating that the CAPS PM_{SSA} ~~gives reliable scattering coefficient measurements for aerosol mixtures and~~ scattering channel~~could~~ be considered as a substitute for the nephelometer scattering measurement~~ and delivers reliable SSA measured simultaneously in one volume of the same instrument~~. Trade-offs in the CAPS PM_{SSA} versus NEPH comparison include the three wavelengths and backscatter measurements of the NEPH versus the single wavelength of the CAPS PM_{SSA}, countered by the additional extinction measurement of the CAPS PM_{SSA} allowing for absorption and SSA values to be simultaneously measured.

~~Instead of using~~In addition to regression analys~~ie~~s, where outliers and/or high values can ~~are~~ dominat~~eing~~ the fitted slope of the regression, ~~-~~ another ~~-~~ ~~more robust~~ statistical ~~analysis~~ approach is to investigate ~~of~~ the ensemble averaged instrumental ratios (σ_{ap} (instrument #1) / σ_{ap} (instrument #2)), which is more sensitive to ~~small~~ errors at low values ~~will be shown in the following section~~. Resulting 630 nm and 450 nm wavelength absorption coefficient ratios are tabulated in Table 5 and 6, respectively. The average ratios are calculated from the points shown in Figure 5 for AQ and AS mixtures and from results obtained for the other absorbing particle types externally mixed with AS particles. ~~For the table 5 – table 6 the ratios are calculated using averaged 1Hz measurement data. The average intervals are adapted for constant conditions, waiting 15 minutes until the production and nephelometer were settled/relaxed lasting for about 5 minutes until the next mixture was setup in the sample line restarting the procedure.~~

Table ~~5~~5. Ensemble average ~~as a~~ ratio~~s~~ of σ_{ap} (TAP) / σ_{ap} (CAPS, NEPH) at 630 nm wavelength. N denotes the number of experiments used for the average.

630 nm wavelength	BC	AQ	SOOT	MB
σ_{ap} (TAP) / σ_{ap} (CAPS,NEPH) ~~with variance~~	1.22 ± 2.57 (N=36)	0.97 ± 0.22 (N=28)	1.10 ± 1.22 (N=25)	0.88 ± 0.17 (N=8)
σ_{ap} (TAP) / σ_{ap} (CAPS,NEPH) for samples with σ_{ap} >10 Mm^{-1} ~~variance~~	1.08 ± 0.19 (N=24)	0.94 ± 0.10 (N=11)	0.86 ± 0.13 (N=6)	-

Table ~~Table Table 5~~5 demonstrate~~s~~ that the light absorption values agree for the different methods in general. With an ensemble average for the ratio σ_{ap} (TAP) / σ_{ap} (CAPS,NEPH) ~~close to 1~~of 0.97 ± 0.22, ~~a~~ good agreement is ~~achieved~~ confirmed with ~~and~~ over 60% of all datapoints for external mixtures of ~~Aquadag~~ AQ and AS ~~fits~~falling within a range of σ_{ap} (TAP) / σ_{ap} (CAPS,NEPH) = {0.8 – 1.2}. These results support the linear regression results in Table 4, though exhibit larger scatter due to the greater sensitivity to small errors at low values.

Formatte

The average ratios for other externally mixed absorbing aerosol types deviate more from unity than AQ mixtures. Most of this scatter can be ascribed to the greater sensitivity of the ratio to small errors at low values. By filtering these ratios ~~Regarding fractal soot particles this ratio deviates most form 1, while using Cabot Black over 50% of all data to fit in the range of σ_{ap} (TAP) / σ_{ap} (CAPS, NEPH) = {0.8 – 1.2}. Filtering these instrument ratios~~ for points with σ_{ap} ~~<~~ > 10 Mm^{-1}~~,~~ ~~the relative frequency distribution shows almost no modal value. Filtering the data for σ_{ap} > 10 Mm^{-1} about~~approximately 80% of ~~these~~ the data are within the range of 0.8-1.2, ~~.~~ The ratios for σ_{ap} < 10 Mm^{-1} exhibited almost no modal value in the relative frequency distributions, confirming that scatter in low values significantly affects the average ratios.

~~The Filtering is done by excluding this low values as soon the σ_{ap} surpasses this for any wavelength. For each experiment run a different aerosol mixture was generated with different overall extinction levels. We used a 100 sec average (1 HZ sampling rate) per run, after the nephelometer reached a steady state. N denotes the number of experiments used for the average. 100 seconds were chosen to fit a minimum of data uncertainty and detection limits shown in Allan plots by {Massoli, 2010 for the CAPS extinction measurement and {Ogren, 2017 for the TAP. Averaging for longer periods would increase variance values of TAP or CAPS regarding the long-term drifts due to transmission (TAP) and baseline drift (CAPS).#230}#72}~~

Table ~~6~~6. Ensemble average ratios of σ_{ap} (TAP) / σ_{ap} (CAPS, NEPH) at 450 nm wavelength. N denotes the number of experiments used for the average.~~Ensemble averages as a ratio of σ_{ap} (TAP) / σ_{ap} (CAPS, NEPH) at 450 nm wavelength.~~

450 nm wavelength	BC	AQ	SOOT	MB
σ_{ap} (TAP) / σ_{ap} (CAPS,NEPH) ~~with variance~~	1.03 ± 1.72 (N=36)	1.06 ± 0.38 (N=28)	0.89 ± 1.05 (N=25)	1.28 ± 2.91 (N=8)
σ_{ap} (TAP) / σ_{ap} (CAPS,NEPH) for samples with σ_{ap} >10 Mm^{-1} ~~variance~~	1.08 ± 0.33 (N=24)	1.01 ± 0.13 (N=11)	0.84 ± 0.27 (N=6)	-

Redoing this analysis for 450 nm wavelength, the light extinction and scattering of smaller particles increases compared to the values at 630 nm wavelength. As a result, the errors in calculating the 450 nm wavelength absorption coefficients from the Differential Method also increase. ~~this also increases also the errors associated with the differential method, since, which we observed accordingly.~~ As demonstrated in Table ~~Table 6~~6, only the variance for the ratio σ_{ap} (TAP) / σ_{ap} (CAPS, NEPH) for ~~spherical~~ compact AQ particles ~~deviate less from unity~~was less than 1 (i.e., <100%), with over 50% of the data being within the range of 0.8-1.2. ~~Still, all~~All ensemble average ratios~~s~~ wea~~r~~re close to 1; however, ~~but~~ with an associated error of up to ±1.7 (i.e., ±170%), these values are not significant, which means~~,~~ that the ratios scatter widely with no clear modal value.

Again, filtering the 450 nm data for~~Again filtering~~ ~~only for~~ σ_{ap} >10 Mm^{-1} greatly improves the results, ~~the methods agree well~~ with ~~significant~~ ratios σ_{ap} (TAP) / σ_{ap} (CAPS, NEPH) =1.08 ± 0.33 for BC. The best instrumental ratio ~~with~~ of 1.01 ± 0.13 is shown for AQ mixtures in Table 6 at 450 nm wavelength.

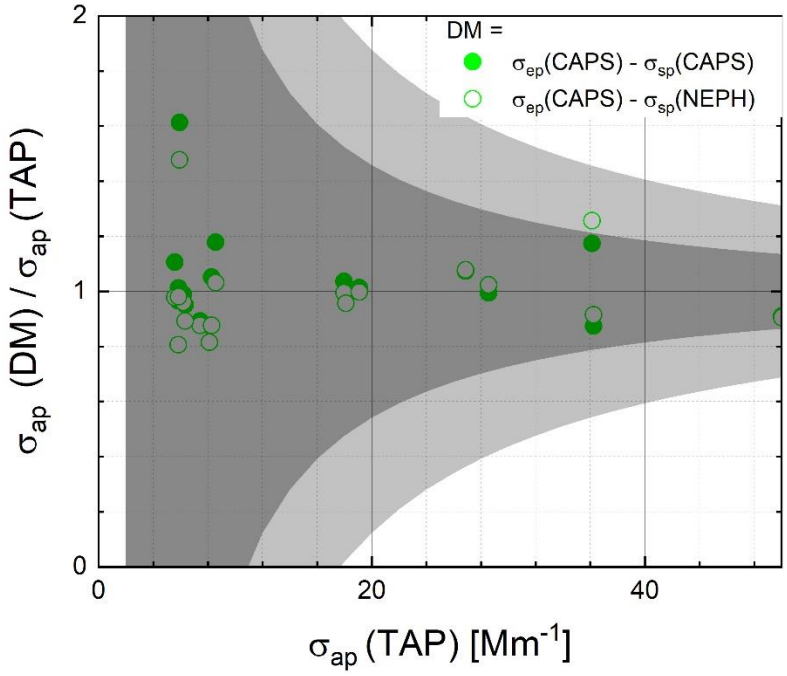
DM =
σep(CAPS) - σsp(CAPS)
σep(CAPS) - σsp(NEPH)
σap (DM) / σap (TAP)
σap (TAP) [Mm-1]
0
1
2
0
20
40

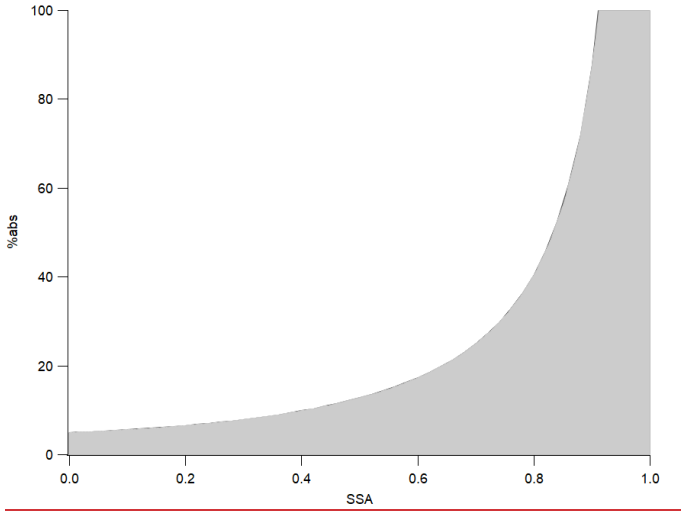
%abs
SSA
0
20
40
60
80
100
0.0
0.2
0.4
0.6
0.8
1.0

580

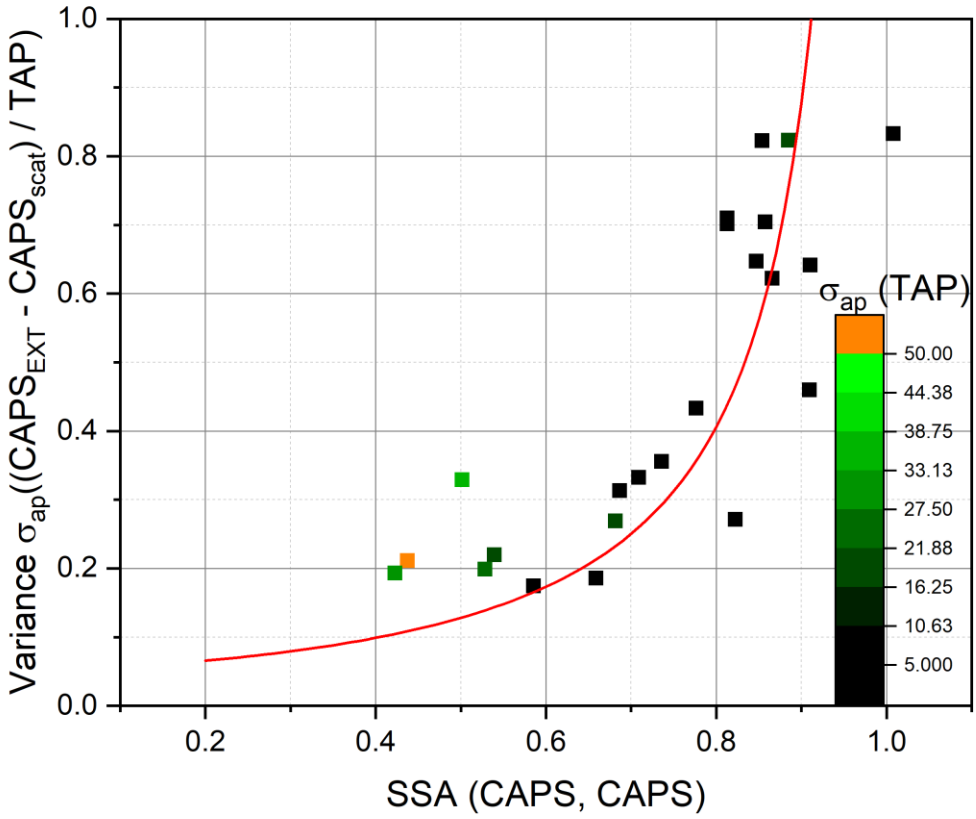

Figure 6. ~~Ratios~~Variance of the measured absorption coefficients [σ_{ap} (~~DM~~CAPS, CAPS)) / σ_{ap} (TAP)] for ~~F~~f~~or~~ ~~b~~Both ~~D~~differential M~~m~~ethod~~s~~ calculation~~ss~~ relative to TAP ~~measurements, the absorption coefficient σ_{ap} (DM) = {σ_{ap} (CAPS,CAPS) see filled symbols, and σ_{ap} (DM) = σ_{ap} (CAPS,NEPH) see open symbols,} the rations of σ_{ap} (DM) / σ_{ap} (TAP)for~~measurements for AQ and AS external mixtures ~~Aquadag aerosol type mixtures as function of σ_{ap}(TAP) are shown~~. The ratios are plotted against the aerosol measured SSA values [SSA(~~NEPH~~CAPS, CAPS)]. ~~The dark grey error band~~ The red line represents the calculated relative errors using Gaussian error propagation of the uncertainties of the DM Method with 1 as 100%.~~assuming σ_{ep} =50 Mm^{-1}; the light grey error band represents calculated relative errors assuming constant σ_{ep} = 200 Mm^{-1}~~.

In order to demonstrate the dependency of the uncertainties associated with the Differential Methods for deriving σ_{ap} values on the SSA, the ensemble ~~averaged~~variance ratios of ~~on the magnitude of σ_{ap} the instrumental ratios of σ_{ap} (TAP) / σ_{ap} (CAPS, NEPH) / σ_{ap} (TAP) and~~ σ_{ap} (CAPS, CAPS) / σ_{ap} (TAP) ~~/ σ_{ap} (CAPS, CAPS)~~ are shown as functions of ~~σ_{ap} (TAP)~~SSA in Figure 6~~Figure 6Figure 6~~. For ~~σ_{ap}~~ SSA values ~~lower~~ greater than ~~20 Mm^{-1}~~0.9, light absorption coefficients derived for the DM methods have ~~errors~~ propagated uncertainties ~~even~~ over 100% independently of their load.~~ for light absorption coefficient are derived for the DM methods assuming for σ_{ep} = 200 Mm^{-1}~~. The experimental

Formatte

data ~~stays fall~~align within these~~is~~ calculated relative uncertainties~~y~~. ~~For σ_{ap} values over 50 Mm^{-1}, the instrumental ratio deviates from 1 less than 10-20%. Both differential methods show an excellent agreement with each other on a point by point basis as already demonstrated in Figure 5Figure 5 thus, open and filled marks representing the two different methods are always in close proximity.~~

Table ~~7~~7. Linear regression results of scattering, σ_{sp}, extinction, σ_{ep}, and absorption, σ_{ap}, coefficients for external mixtures of BC and AS particles, given as slopes (m), Pearson R, and y-axis intercepts (b). ~~Linear regression analysis of attenuation coefficients using Cabot Black and ammonium sulphate mixtures are shown. Presenting: the slope (m), Pearson (r) and y-axis intersection (b) for different instruments combinations.~~

BC	σ_{sp}(CAPS) vs σ_{sp}(NEPH)	$\sigma_{sp(CAPS,TAP)}$ vs. $\sigma_{sp(NEPH)}$	$\sigma_{ep(TAP,NEPH)}$ vs $\sigma_{ep(CAPS)}$	$\sigma_{ap(TAP)}$ vs. $\sigma_{ap(CAPS,NEPH)}$
		630 nm		
m	1.02 ± 0.03	0.99 ± 0.05	0.94 ± 0.02	0.90 ± 0.02
~~r~~R	0.98	0.96	0.99	0.99
b [Mm^{-1}]	-0.69±0.7	-2.13 ± 1.01	3.59 ± 0.60	2.57 ± 0.11
		450 nm		
m	0.99 ± 0.02	1.06 ± 0.06	0.94 ± 0.03	0.86 ± 0.05
~~r~~R	0.99	0.95	0.98	0.97
b [Mm^{-1}]	5.36 ± 1.45	-0.59 ± 3.86	0.97 ± 3.17	2.98 ± 0.48

Table ~~8~~8. Linear regression results of scattering, σ_{sp}, extinction, σ_{ep}, and absorption, σ_{ap}, coefficients for external mixtures of SOOT and AS particles, given as slopes (m), Pearson R, and y-axis intercepts (b). ~~Linear regression analysis attenuation coefficients slopes for fresh combustion soot and ammonium sulphate mixtures given as slopes (m), Pearson (r) and y-axis intersection (b).~~

SOOT	σ_{sp}(CAPS) vs σ_{sp}(NEPH)	$\sigma_{sp(CAPS,TAP)}$ vs. $\sigma_{sp(NEPH)}$	$\sigma_{ep(TAP,NEPH)}$ vs $\sigma_{ep(CAPS)}$	$\sigma_{ap(TAP)}$ vs. $\sigma_{ap(CAPS,NEPH)}$
		630 nm		
m	1.06 ± 0.04	0.9 ± 0.20	0.99 ± 0.08	0.76 ± 0.11
~~r~~R	0.99	0.74	0.97	0.92
b [Mm^{-1}]	0.05 ± 0.56	1.57 ± 3.21	1.80 ± 1.72	3.93 ± 1.68
		450 nm		

m	0.81 ± 0.03	0.77 ± 0.07	0.92 ± 0.04	0.70 ± 0.10
~~r~~R	0.99	0.97	0.98	0.91
b [Mm^{-1}]	1.73 ± 0.45	2.64 ± 0.91	3.26 ± 2.24	1.75 ± 0.82

Table ~~9~~9. Linear regression results of scattering, σ_{sp}, extinction, σ_{ep}, and absorption, σ_{ap}, coefficients for external mixtures of MB and AS particles, given as slopes (m), Pearson R, and y-axis intercepts (b). ~~Linear regression analysis of volumetric cross sections slopes of the acrylic paint (Magic Black (MB)) and ammonium sulphate mixtures given as slopes, Pearson R and y-axis intersection.~~

MB	σ_{sp}(CAPS) vs σ_{sp}(NEPH)	$\sigma_{sp(CAPS,TAP)}$ vs. $\sigma_{sp(NEPH)}$	$\sigma_{ep(TAP,NEPH)}$ vs $\sigma_{ep(CAPS)}$	$\sigma_{ap(TAP)}$ vs. $\sigma_{ap(CAPS,NEPH)}$
		630 nm		
m	0.96 ± 0.03	1.05 ± 0.03	0.96 ± 0.03	0.57 ± 0.10
~~r~~R	0.99	0.99	0.99	0.94
b [Mm^{-1}]	0.42 ± 0.79	-0.95 ± 0.53	0.99 ± 0.51	1.06 ± 0.38
		450 nm		
m	1.02 ± 0.02	1.00 ± 0.16	0.89 ± 0.11	0.21 ± 0.14
R~~r~~	0.99	0.95	0.97	0.58
b [Mm^{-1}]	-1.85 ± 0.78	-0.82 ± 6.04	4.58 ± 4.88	3.43 ± 0.91

The linear regression analyse~~i~~s reporting fitted slopes, Pearson coefficients, and y-offsets for attenuation coefficients for external mixtures of AS and ~~the~~ the different light absorbing aerosol types are presented in Table ~~Table Table 7~~7 (BC), Table ~~Table Table 8~~8 (~~soot~~SOOT), and Table ~~Table Table 9~~9 (MB). ~~In general, for~~For 630 nm wavelength results, high Pearson ~~rates~~ coefficients (R~~r~~>0.~~,~~96) with negligible offsets (b<1 Mm^{-1}) and slopes ranging from 0.90 to 1.05 demonstrate~~s~~ ~~a~~ good agreement (i.e., closure) for scattering and extinction coefficient measurements. Especially for MB and ~~Soot~~SOOT, the TAP measurements tend to overshoot the Differential method ~~tends to underestimate the~~ value ~~compared to TAP measurements~~ by 20-~~-~~40 %, whereas for BC the difference is only 10%. The reason could be that soot is a fractal agglomerate and in-situ methods as well as filter-based methods give different results as a function of the primary particle size (Sorensen et al., 2010~~p~~) as well as of the previous mentioned filter-based artifacts, including changes of the slope at higher σ_{ap} (TAP) values. We measured values for BC ranging from 14 to 400 Mm^{-1} for $\sigma_{ep,630nm}$, 1 to 322 Mm^{-1} for $\sigma_{ap,630nm}$, and 12 to 174 Mm^{-1} for $\sigma_{sp,630nm}$. For SOOT, we measured values ranging from 12 to 158 Mm^{-1} for $\sigma_{ep,630nm}$, 1 to 322 Mm^{-1} for $\sigma_{ap,630nm}$, and 5 to 80 Mm^{-1} for $\sigma_{sp,630nm}$.

For 450 nm wavelength results, similar slopes, Pearson R, and y-offset values ~~could be~~are reported ~~for these aerosol types mixtures with ammonium sulphate~~. Linear regression slopes for SOOT ~~Fresh soot particle mixtures values~~ decrease~~ing~~ ~~with~~ at the lower wavelength to a ~~slope~~ value of 0.77 for light scattering ~~intercomparison~~ and ~~σ_{ap} of~~ 0.7

Formatte
Formatte
Formatte

for light absorption. Thisese decrease may well be is as well an effect of the primary particles size of agglomeration, since those relationships changeees with the wavelength.

For Magic BlackMB, the light absorption measurements using the DM method for 450 nm shows the highest difference compared to the TAP measurement with a regression slope of 0.21 ± 0.14. The reasons could be include different absorption behaviour (i.e., filter-based artifacts) for filter-based method relative to in-situ to filter measurements (Lack, 2008). Unfortunately, and no clear indications understanding of the MB particle shape, phase, or uniformity could be made during this study.

We measured values for BC ranging from 14 to 400 Mm^{-1} for $\sigma_{ep,630}$, 1 to 322 Mm^{-1} for $\sigma_{ap,630}$ and 12 to 174 Mm^{-1} for $\sigma_{sp,630}$. For Soot we measured values ranging from 12 to 158 (one value with 1437 Mm^{-1} excluded from regression analysis) Mm^{-1} for $\sigma_{ep,630}$, 1 to 322 Mm^{-1} for $\sigma_{ap,630}$ and 5 to 80 Mm^{-1} for $\sigma_{sp,630}$.

32.32 Intensive Parameters of Aerosol Mixtures

32.2.1 Single scattering Albedo (SSA)

The Single Scattering Albedo (SSA), as an important climate parameter, is investigated here as a relative measurement using multiple different methods of derivation to determine if closure between the different methods can be achieved. used for instrument validation in this section. To obtain this parameter, different methods are shown in Table 10. Each method excludes at least one instrument from the calculation, thus, instrument intercomparison is possible.

The SSA for different combinations of instruments are derived using Eq. (2) as follows. In the followingwith the instruments used are denoted in parentheses in Equations 7-10.

$$SSA(NEPH,TAP) = \frac{\sigma_{sp}(\mathrm{NEPH})}{\sigma_{ap}(\mathrm{TAP})+\sigma_{sp}(\mathrm{NEPH})} \quad \text{Eq. (7)}$$

$$SSA(CAPS,TAP) = \frac{\sigma_{ep}(\mathrm{CAPS})-\sigma_{ap}(\mathrm{TAP})}{\sigma_{ep}(\mathrm{CAPS})} \quad \text{Eq. (8)}$$

$$SSA(CAPS,CAPS) = \frac{\sigma_{sp}(\mathrm{CAPS})}{\sigma_{ep}(\mathrm{CAPS})} \quad \text{Eq. (9)}$$

As reference we use the following often used combination:

$$SSA(NEPH,CAPS) = \frac{\sigma_{sp}(\mathrm{NEPH})}{\sigma_{ep}(\mathrm{CAPS})} \quad \text{Eq. (10)}$$

We have chosen to use the SSA(NEPH, CAPS) derived SSA values as a reference for these studies, as this method This allows us to test the CAPS measured SSA with an in-dependent, establisheddd method, which is used for example in ((Sheridan, 2005))as a reference with the nephelometer and another cavity ring down method delivering aerosol light extinction values. However, a strong argument could be made that the CAPS PM_{SSA} Monitor derived SSA values should be the true reference here, as It is a clear advantage, that the CAPSssa Monitors can give the CAPS-derived SSA values were obtained by simultaneously measuring the scattering and extinction of same airaerosol sample within a single instrument at the same time with the volume. #39}

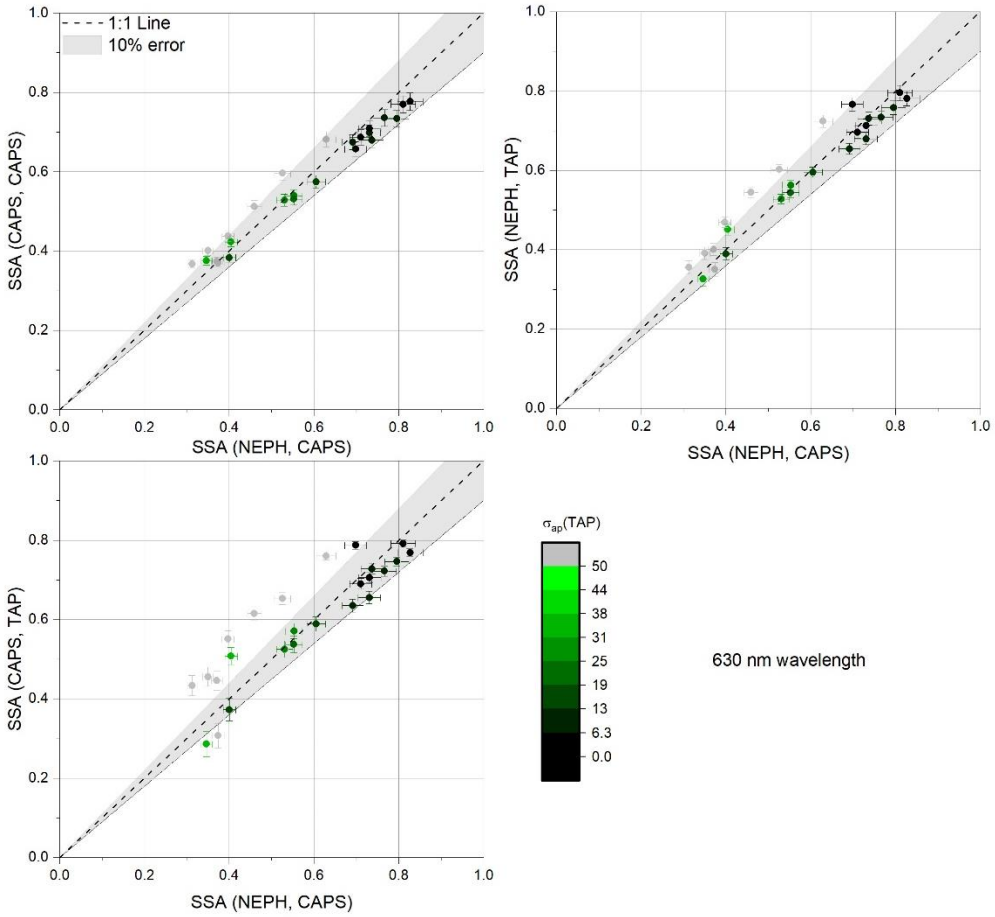
1:1 Line
10% error
SSA (CAPS, CAPS)
SSA (NEPH, CAPS)
SSA (NEPH, TAP)
SSA (NEPH, CAPS)
SSA (CAPS, TAP)
SSA (NEPH, CAPS)
σap(TAP)
50
44
38
31
25
19
13
6.3
0.0
630 nm wavelength

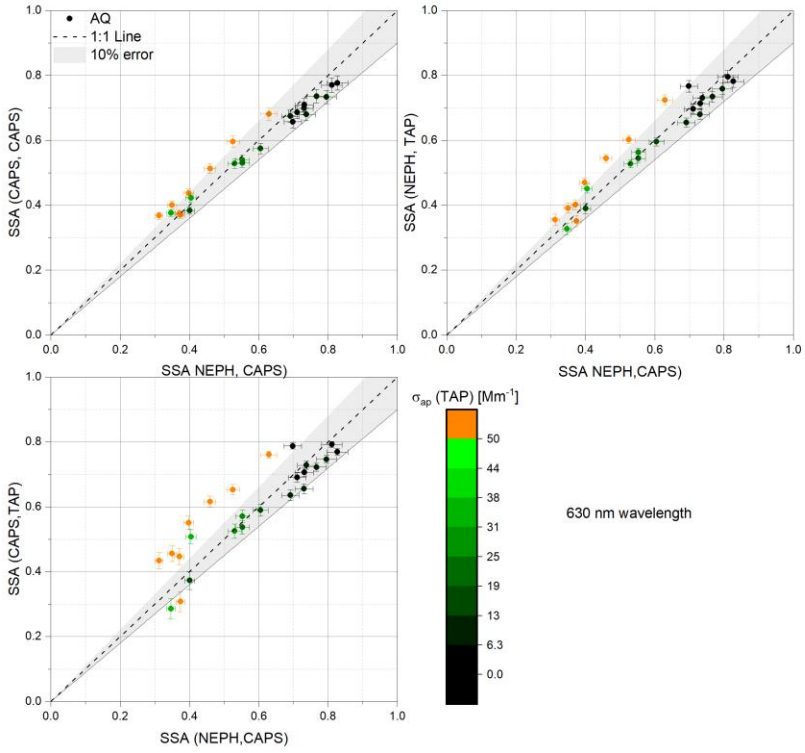

740 **Figure 7.** ~~This figure shows s~~Scatter plots of derived SSA ~~Instrument-to-instrument measurement ratios~~values from various combinations of measurements ~~for~~ at 630 nm wavelength ~~reported~~ obtained for AQ/AS mixtures (y-axis) versus SSA(NEPH, CAPS) as the reference on the x-axis. ~~(see Equations 7-11.~~ The colour code indicates σ_{ap}(TAP) values shown in Mm^{-1}.

745 Figure 7~~Figure 7~~Figure 7 shows the SSA ~~parameters~~ values obtained by the three combinations of ~~instruments~~ measurements ~~for~~ at 630 nm wavelength. The correlations show~~s~~ reasonable results ~~within~~ relative to a ~~±+~~ 10% error band, with the best correlation obtained for the SSA(CAPS, CAPS) versus SSA(NEPH, CAPS) measurements. In general, the higher the SSA values, the lower the measured absorption coefficients, σ_{ap}, ~~Spotting for dark colours in the colour code – Low σ_{ap} values are only seen for SSA >0.6 as expected~~ reflecting that there are just fewer particles
750 of Aquadag in the external aerosol mixture. The exception to this trend and the points exhibiting the greatest number of outliers (>10% from 1:1 line) are the points with ~~General, the load of absorbing particles seems not to not influence the accuracy of the method, except for~~ high absorption coefficients (~~>over~~ 50 Mm^{-1}~~.~~). ~~Here, t~~The largest outliers are observed in the instrument combinations that include the TAP and may be due to ~~TAP shows~~ a nonlinear response in the TAP under high aerosol loadings~~which is visible in Figure 7 as offset of 0.1 higher than the SSA reference calculated using Eq. (10)~~.
755

~~Like~~ Similar~~ly~~ to ~~in~~ the previous section, we calculated the ensemble ~~average~~ (average ~~of~~ instrument-to-instrument measurement ratio averages~~s~~, using the SSA(NEPH, CAPS) values for reference, as another way of examining the

correlations.) was calculated to show a robust measure for the overall agreement of this parameter. In Table 10 tThe SSA values for all absorbing aerosol types (externally mixed with AS) are summarized in Table 10. We use The nephelometer and CAPS extinction was used again as referencefor reference once again. The highest largest variance deviation is visible with combustion soot for TAP related data. The deviations of the reported mean from 1 are less than the relative uncertainties which range around 0.09.

Table 1010. Ensemble average of instrument-to-instrument measurement ratio averages and standard deviationss for different instrument combinations used to derive to obtain the SSA values at 630 nm wavelength using $SSA(NEPH, CAPS)$ as reference.

Instrument combinations used for SSA calculations	BC	AQ	SOOT	MB
SSA (CAPS, CAPS) / $SSA(NEPH, CAPS)$	1.00 ± 0.08	1.01 ± 0.07	1.07 ± 0.07	1.00 ± 0.04
$SSA(NEPH, TAP)$ / $SSA(NEPH, CAPS)$	0.96 ± 0.08	1.02 ± 0.08	1.04 ± 0.29	1.00 ± 0.03
$SSA(CAPS, TAP)$ / $SSA(NEPH, CAPS)$	0.98 ± 0.16	1.05 ± 0.16	1.07 ± 0.51	1.00 ± 0.03

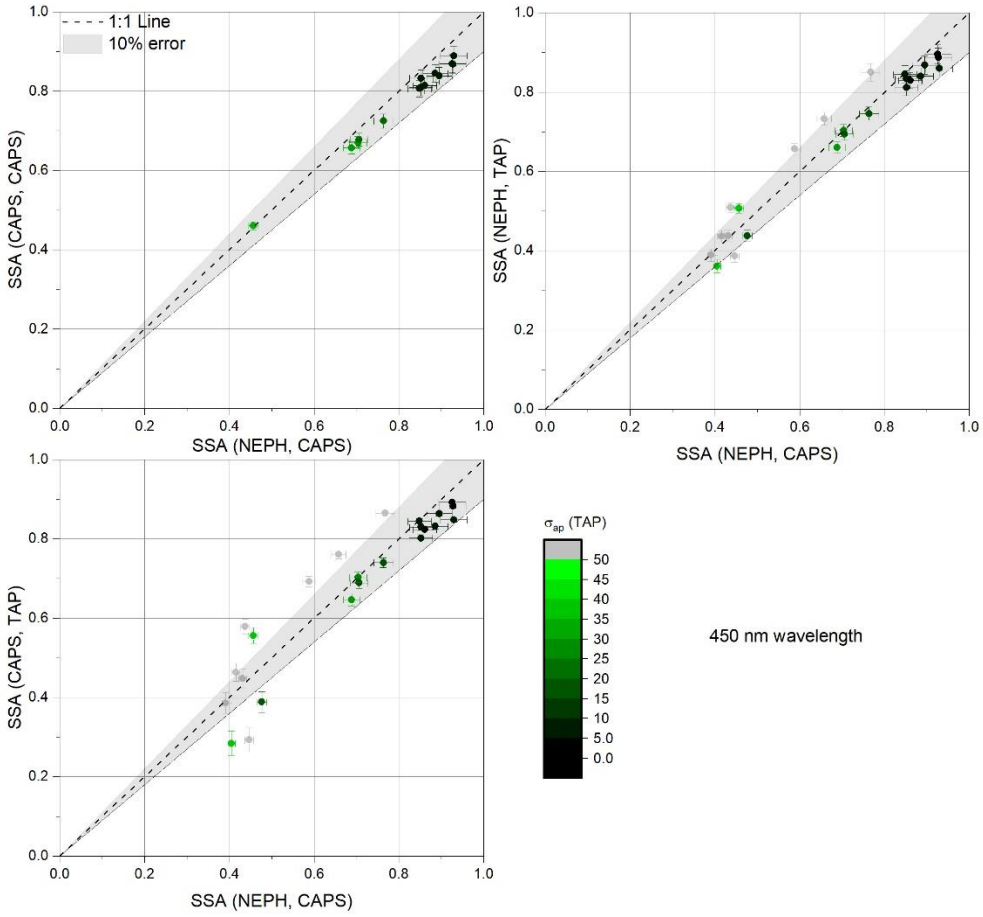
1:1 Line
10% error
SSA (CAPS, CAPS)
SSA (NEPH, CAPS)
SSA (NEPH, TAP)
SSA (NEPH, CAPS)
SSA (CAPS, TAP)
SSA (NEPH, CAPS)
σap (TAP)
50
45
40
35
30
25
20
15
10
5.0
0.0
450 nm wavelength

770

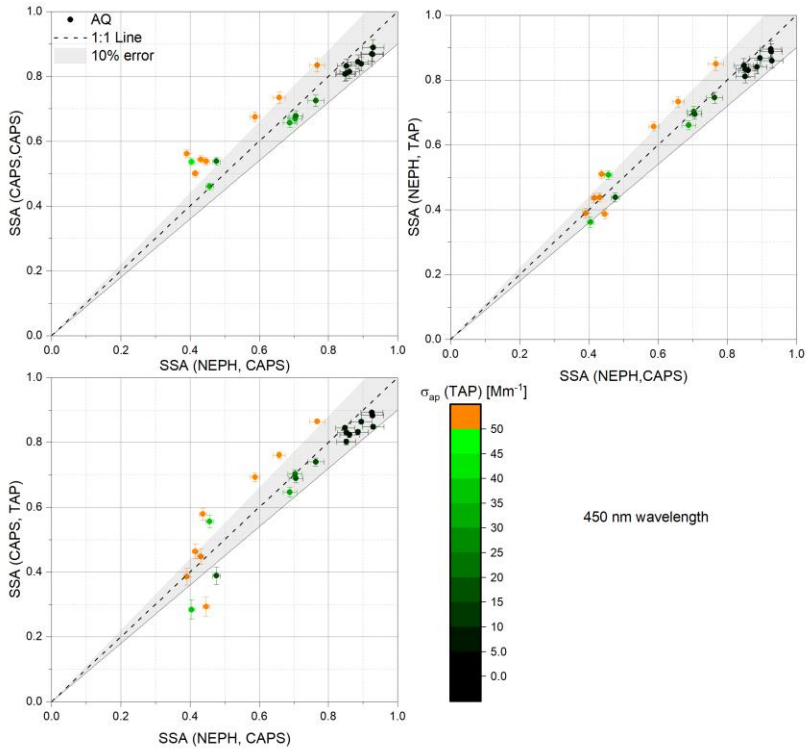

790 **Figure 8.** ~~This figure shows s~~Scatter plots of ~~Instrument-to-instrument ratios for~~Differential Method derived ~~the~~ SSA ~~for~~ values for different instrument combinations at 450 nm wavelength using AQ/AS mixtures versus ~~for different instrument combinations as functions of the references~~ SSA ~~(~~NEPH, CAPS). The colour code indicates σ_{ap}(TAP) values shown in Mm^{-1}.

795 Figure 7~~Figure~~ 8 shows the SSA values obtained by the three combinations of measurements at 450 nm wavelength for all AQ/AS external mixtures. ~~Figure 8 presents scatter plots of Instrument-to-instrument ratios for the SSA values for 450 nm wavelength using AQ/AS mixtures for all instrument combinations.~~ Observed patterns are comparable to the 630 nm wavelength results ~~of~~ in Figure 7~~Figure 7Figure 7 for 630 nm wavelength~~. For absorption coefficients up to 50 Mm^{-1}, all methods agree within 10%. Above 50 Mm^{-1}~~,~~ ~~again~~ the largest outliers are again observed in the 800 instrument combinations that include the TAP instrument~~non-linear response of TAP is visible again showing an offset of 0.1 for the instrument-to-instrument ratio~~.

Formatte

Formatte

Table ~~11~~11. Ensemble instrument-to-instrument measurement ratio averages and standard deviations for different instrument combinations used to derive SSA values at 450 nm wavelength using $SSA(NEPH, CAPS)$ as 805 reference.~~Ensemble averages of instrument-to-instrument measurement ratios for different instrument combination to obtain the SSA at 450 nm wavelength using $SSA(NEPH, CAPS)$ as reference (see Eq. 7-10).~~

Instrument combination used for SSA calculation	BC	AQ	SOOT	MB
SSA (CAPS, CAPS) / $SSA(NEPH, CAPS)$	1.17 ± 0.21	1.04 ± 0.13	1.11 ± 0.13	0.98 ± 0.02
SSA (NEPH, TAP) / $SSA(NEPH, CAPS)$	1.07 ± 0.08	1.02 ± 0.08	0.96 ± 0.19	1.04 ± 0.13
SSA (CAPS, TAP) / $SSA(NEPH, CAPS)$	1.11 ± 0.13	1.03 ± 0.14	0.64 ± 0.38	1.05 ± 0.14

Table 11 summarizes the 450 nm wavelength ensemble instrument-to-instrument measurement ratio averages, using the SSA(NEPH, CAPS) values for reference. The pattern~~,~~ that ~~more~~ fractal aerosol optical properties appear to~~s~~ differ most from the ~~ensemble average~~reference values as the wavelength decreases is visible here, too. The fresh combustion soot aerosol shows ~~with 0.64 ± 0.38 highest~~ the largest deviation from 1 (0.64 ± 0.38) for SSA (CAPS, TAP) measurements. But, overall, all the instrument-to-instrument ratios are ~~close to~~ unity within the observed variances.

~~3~~2.~~2~~3.2 Ångström E~~e~~xponents~~: EAE~~

~~In this section, we will now focus on the next important and climate model relevant aerosol parameter. The~~ Ångström exponents are calculated from extensive parameters ~~of~~ measured at different wavelengths. Even a small ~~precision~~ error in the extensive parameter measurements can result~~s~~ in a ~~high~~ significant ~~deviation~~uncertainty in the derived Ångström exponents, considering error propagation. Some of optical instruments used in the current study operated at slightly different wavelengths, such that the derived Ångström exponents will exhibit slight biases due to these wavelength difference; these biases are small relative to the observed variances and are thus assumed negligible. ~~To demonstrate the overall variability, all aerosol types measured are shown simultaneously in all plot in this section.~~

The following equations, based on Eq.(3), are used to derive the Angström exponents for extinction, scattering, and absorption using different i~~I~~nstrument combinations with their specific wavelengths indicated:

$$xAE(\text{Instrument1}, \text{Instrument 2}) = -\frac{\log\left(\frac{\sigma_{xp\lambda1}(\text{Instrument1,Instrument 2})}{\sigma_{xp\lambda2}(\text{Instrument1,Instrument 2})}\right)}{\log(\lambda1/\lambda2)} \quad \text{Eq. (11)}$$

$$\text{EAE}(\text{CAPS}) = -\frac{\log\left(\frac{\sigma_{ep\lambda1}(\text{CAPS})}{\sigma_{ep\lambda2}(\text{CAPS})}\right)}{\log(450/630)} \quad \text{Eq. (12)}$$

$$\text{EAE}(\text{NEPH}, \text{TAP}) = -\frac{\log\left(\frac{\sigma_{ep\lambda1}(\sigma_{ap(\text{TAP})}+\sigma_{sp(\text{NEPH})})}{\sigma_{ep\lambda2}(\sigma_{ap(\text{TAP})}+\sigma_{sp(\text{NEPH})})}\right)}{\log(450/630)} \quad \text{Eq. (13)}$$

$$\mathrm{SAE(NEPH)} = -\frac{\log\left(\frac{\sigma_{sp\lambda1}(\mathrm{NEPH})}{\sigma_{sp\lambda2}(\mathrm{NEPH})}\right)}{\log(450/700)} \quad \text{Eq. (14)}$$

$$\mathrm{SAE(CAPS,TAP)} = -\frac{\log\left(\frac{\sigma_{sp\lambda1}(\sigma_{ep}(\mathrm{CAPS})-\sigma_{ap}(\mathrm{TAP}))}{\sigma_{sp\lambda2}(\sigma_{ep}(\mathrm{CAPS})-\sigma_{ap}(\mathrm{TAP}))}\right)}{\log(450/630)} \quad \text{Eq. (15)}$$

$$\mathrm{AAE(TAP)} = -\frac{\log\left(\frac{\sigma_{ap\lambda1}(\mathrm{TAP})}{\sigma_{ap\lambda2}(\mathrm{TAP})}\right)}{\log(467/652)} \quad \text{Eq. (16)}$$

$$\mathrm{AAE(CAPS,NEPH)} = -\frac{\log\left(\frac{\sigma_{ap\lambda1}(\sigma_{ep}(\mathrm{CAPS})-\sigma_{sp}(\mathrm{NEPH}))}{\sigma_{ap\lambda2}(\sigma_{ep}(\mathrm{CAPS})-\sigma_{sp}(\mathrm{NEPH}))}\right)}{\log(450/630)} \quad \text{Eq. (17)}$$

3.2.3 Extinction Ångström Exponents (EAE)

The derived EAE(NEPH, TAP) and EAE(CAPS) values are shown in Figure 9 as a scatter plot and in Figure 10 as a ratio versus the 630 nm wavelength SSA(NEPH, CAPS) values. The EAE(CAPS) values were used as the reference measurement. When directly comparing EAE(NEPH, TAP) to EAE(CAPS), the EAE values agree within 10% variance. The highest measured EAE values for the AQ and AS mixtures, ~3, were close to the EAE values measured for the pure AS particles distributions with CMD ~ 40 nm (Table 3).

The measured EAE(NEPH, TAP) / EAE(CAPS) ratios exhibited no systematic dependence on the σ_{ap}

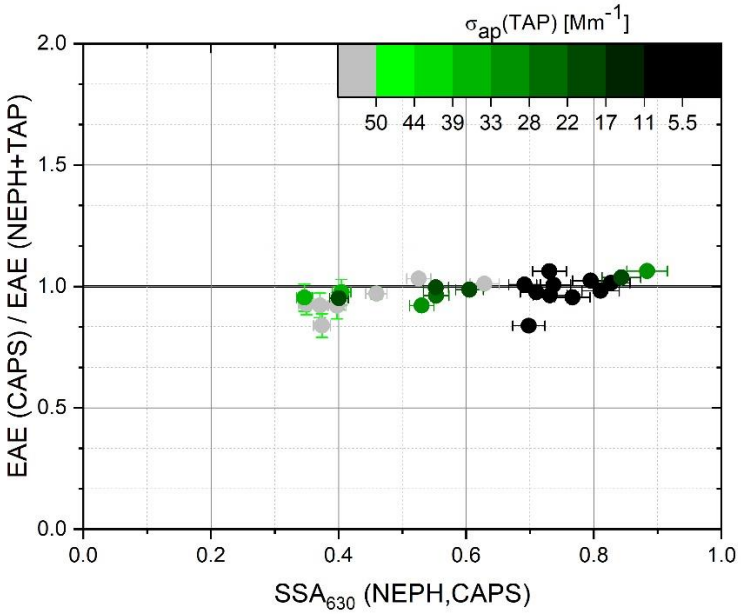

Figure 9. This figure shows the ratio of the extinction Ångström exponent EAE(CAPS) / EAE(NEPH, TAP) as function of SSA(CAPS, NEPH) at 630nm wavelength and the light absorption coefficient σ_{ap}(TAP) at 630 nm in the colour code for AQ/AS mixtures.

N(TAP), Figure 9, or SSA(NEPH, CAPS), Figure 10, values. Measured EAE(NEPH, TAP) / EAE(CAPS) ratios for all absorbing aerosol types (externally mixed with AS) are listed in Table 12. either the SSA, nor σ_{ap} show a

~~systematically dependence on the EAE ratios EAE(CAPS) / EAE(NEPH,TAP) . Only method to method ratios for fresh flame soot deviate up to a ratio of 1.5, indicating higher EAE(CAPS) values compared to EAE(NEPH, TAP) visible in Figure 9. Possible explanations for this may be some smaller aerosol bursts which occur while the flame flickers, or the particle shape influencing the measurement accuracy. A possible explanation for this could be that variances in a small timescale are smoothed out by the bigger volume of the Nephelometer compared to the CAPS instrument, where these fluctuations are seen within the timeline.~~

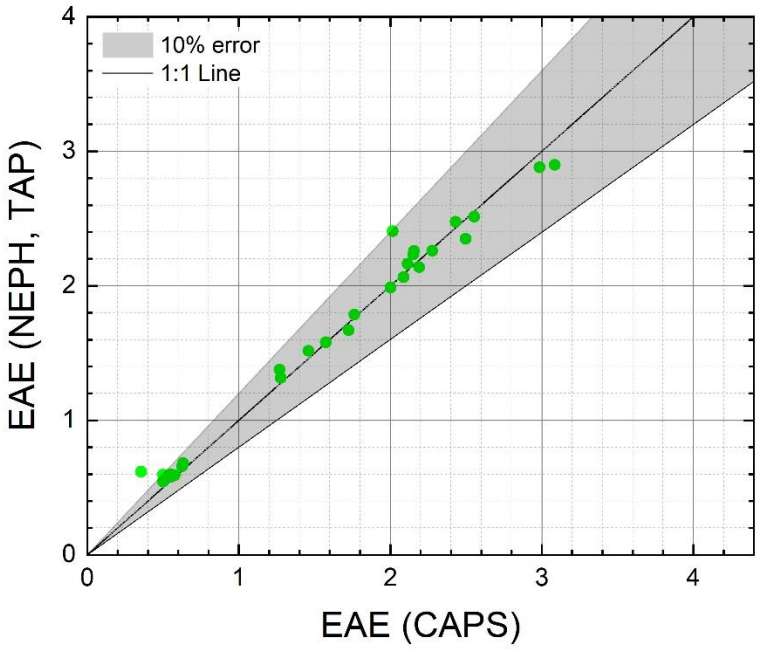
10% error
1:1 Line
EAE (NEPH, TAP)
EAE (CAPS)
0
1
2
3
4

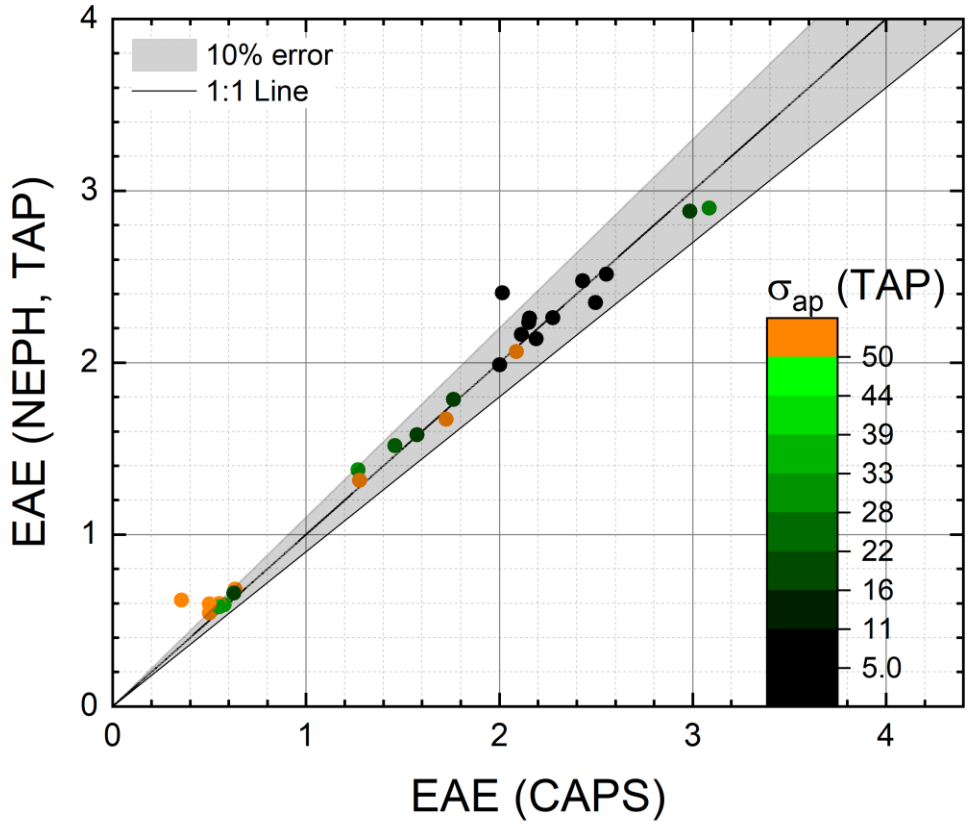
10% error
1:1 Line
EAE (NEPH, TAP)
EAE (CAPS)
σap (TAP)
50
44
39
33
28
22
16
11
5.0
0
1
2
3
4

860

Figure ~~9~~10. Scatter plot of EAE(NEPH, TAP) ~~values~~ measurements compared to EAE(CAPS) ~~obtained by CAPS compared to EAE values obtained from TAP + NEPH~~ measurements ~~showing~~ for AQ/AS mixtures. An error band of 1~~2~~0% is shown.

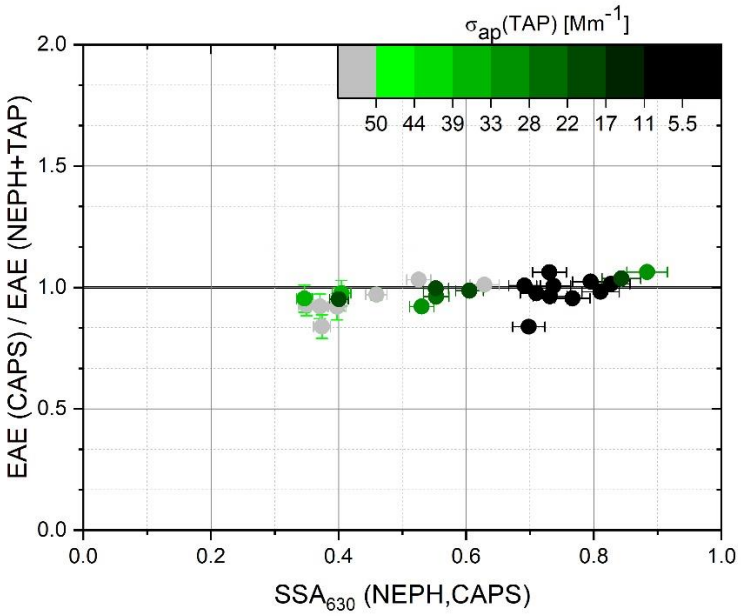

865

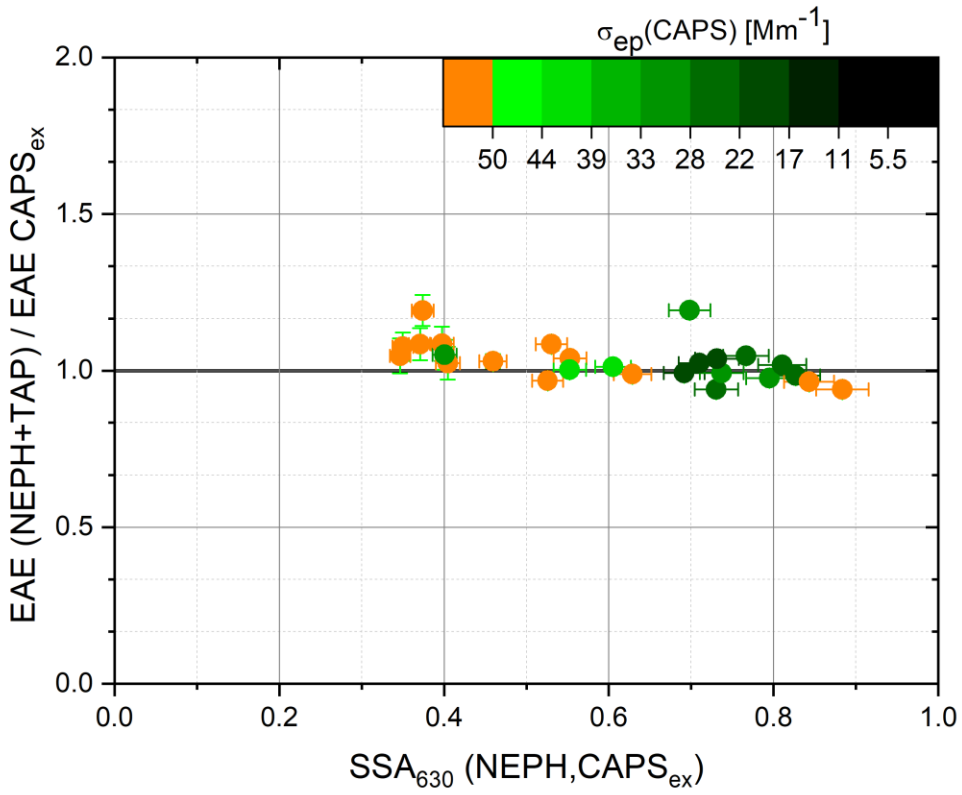

Figure 10. The extinction Ångström exponent EAE(NEPH, TAP) / EAE(CAPS) ratios as a function of 630nm wavelength SSA(NEPH, CAPS) values for AQ/AS mixtures. The 630 nm wavelength light absorption coefficient, σ_{epap}(σ_{epTAP}CAPS), is used as the colour code.

~~When directly comparing EAE(TAP, NEPH) to EAE (CAPS), the EAE values agree within 10% deviation visible in Figure 10. Again, the best correlation is visible with Aquadag mixture particles. For EAE(CAPS) > 2.5 the EAE(TAP, NEPH) tents to underestimate the EAE. Nevertheless EAE(NEPH, TAP) shows the highest values close 3.21 which corresponds to EAE values reported in Table 3 for the pure AS particles which are small in size of about 40nm.~~

~~3.2~~ 3.2 ~~3.4~~ *Scattering Ångström exponent ~~(s: SAE~~)*

The derived SAE(CAPS, TAP) and SAE(NEPH) values are shown in Figure 11 as a scatter plot and in Figure 12 as a ratio versus the 630 nm wavelength SSA(NEPH, CAPS) values. The SAE(NEPH) values were used as the reference measurement. All SAE(CAPS, TAP) and SAE(NEPH) values agree within 10% variance and the measured SAE(CAPS, TAP) / SAE(NEPH) ratios exhibited no systematic dependence on the σ_{sap}(~~TAP~~CAPS), Figure 11, or SSA(NEPH, CAPS), Figure 12, values. The measured SAE(CAPS, TAP) / SAE(NEPH) ratios for all absorbing aerosol types (externally mixed with AS) are listed in Table 12.

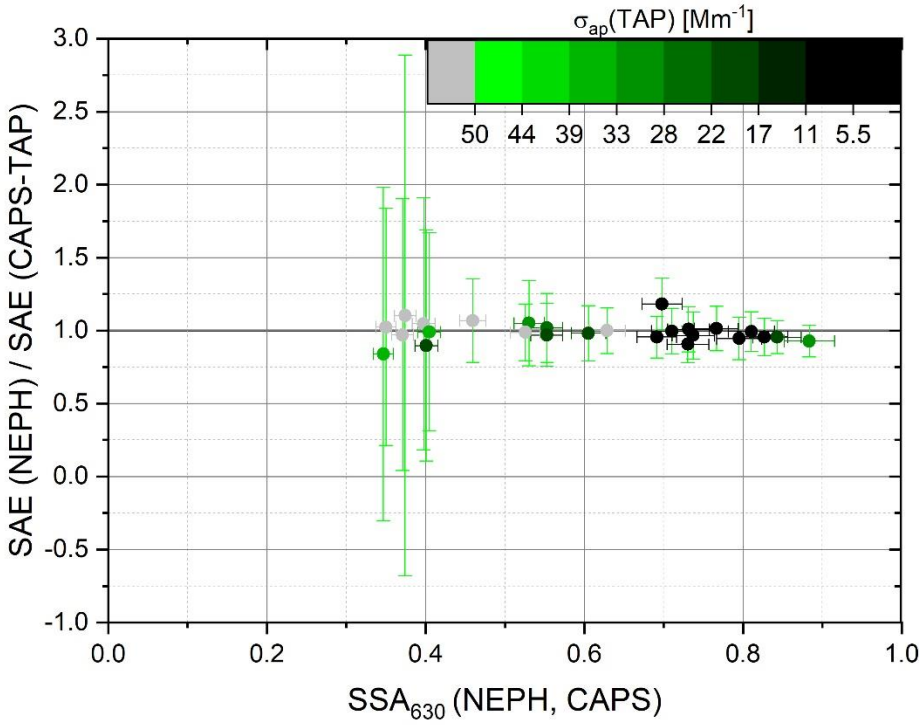

~~C8~~ C8

~~**Figure 11.** This figure shows the instrument to instrument ratio of the Scattering Ångström exponent SAE(NEPH) / SAE(CAPS, TAP) as function of SSA(CAPS, NEPH) wavelength and as function of σ_{ap}(TAP) as a colour code both for at 630 nm.~~

~~The instrument-to-instrument ration of SAE were calculated for each particle type. Most data points show a ratio of close to 1 not biased by σ_{ap} or by the SSA shown in and Figure 11.~~

~~Looking for the instrument-to-instrument SAE ratios for the different absorbing species individually in Table 12, only soot shows an instrument-to-instrument ratio of about 1.43+ 0.61, which, is statistical, is not significant significantly different from 1.~~

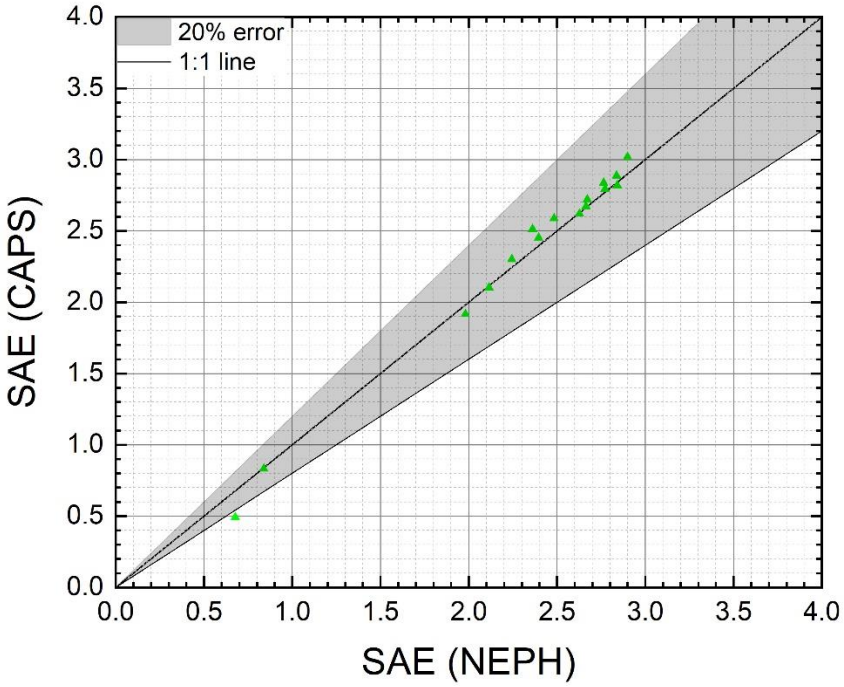
20% error
1:1 line
SAE (CAPS)
SAE (NEPH)
0.0
0.5
1.0
1.5
2.0
2.5
3.0
3.5
4.0

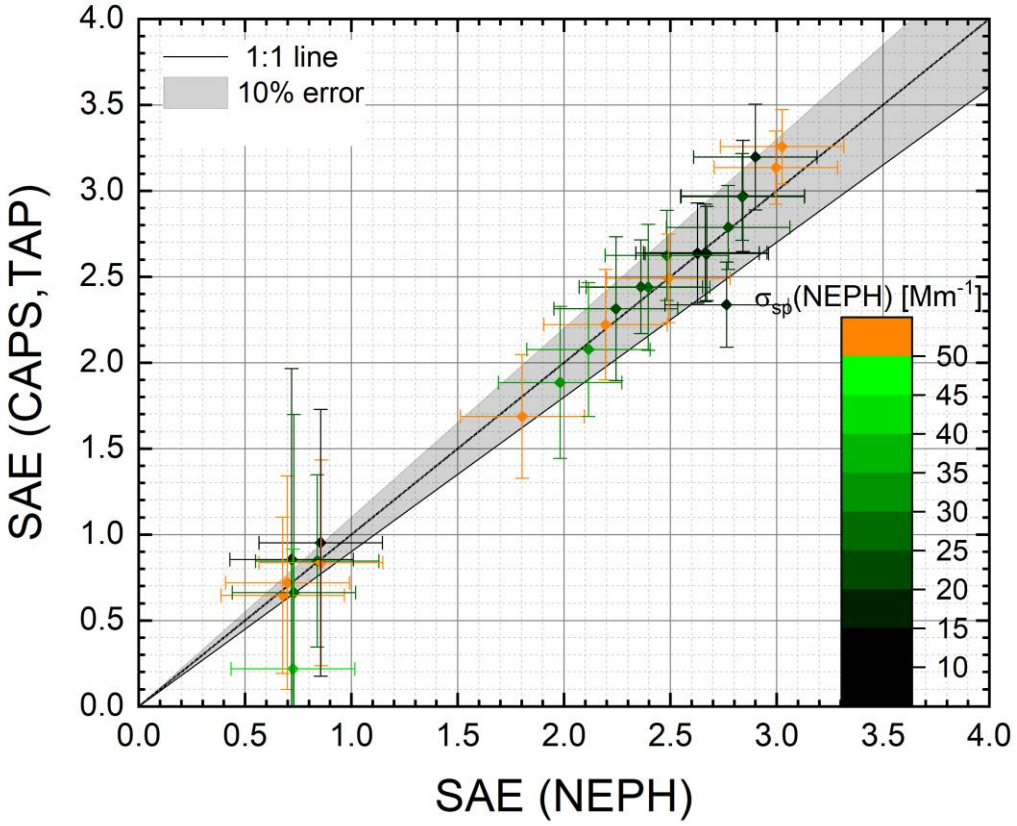

Figure 9~~12~~1. Scatter plot of SAE(~~CAPS~~CAPS,TAP) measurements compared to SAE(NEPH) measurements for AQ/AS mixtures. An error band of 1~~2~~0% is shown.

~~Scatter plot of SAE values obtained by CAPS is compared to SAE values obtained by NEPH for AQ/AS mixtures.~~

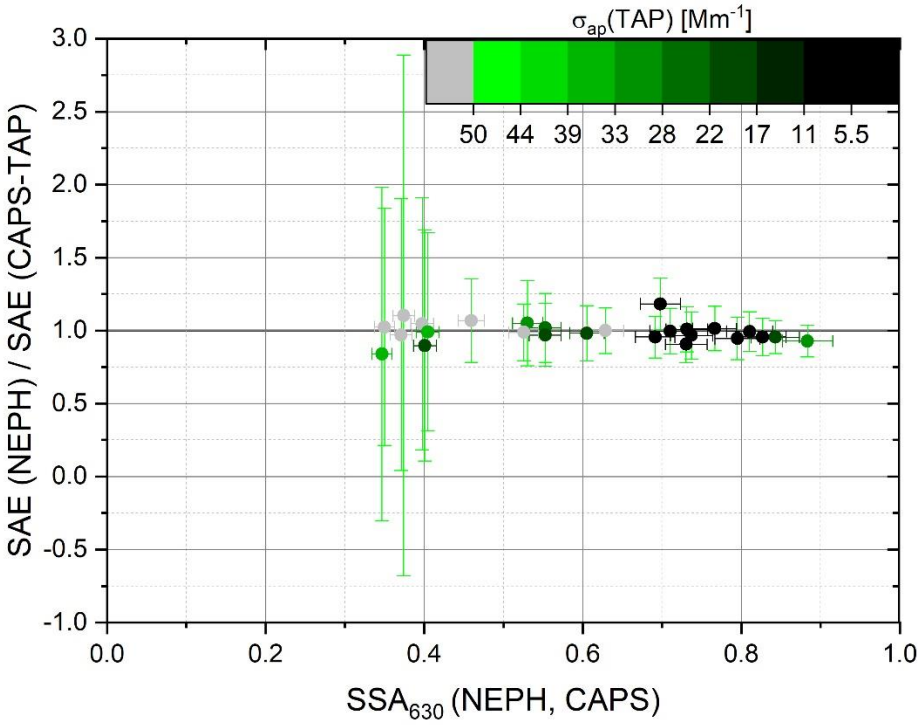
σap(TAP) [Mm-1]
50 44 39 33 28 22 17 11 5.5
SAE (NEPH) / SAE (CAPS-TAP)
SSA630 (NEPH, CAPS)

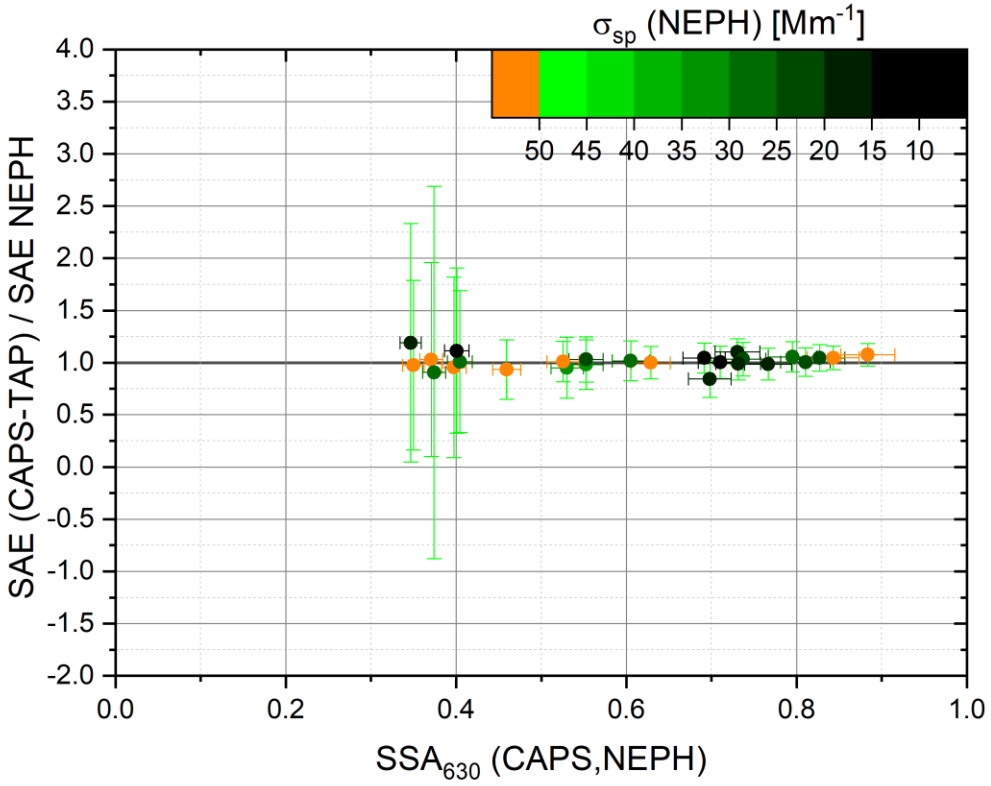
σsp (NEPH) [Mm-1]
50 45 40 35 30 25 20 15 10
SAE (CAPS-TAP) / SAE NEPH
SSA630 (CAPS,NEPH)

Figure 10~~1~~2. The scattering Ångström exponent ratio, SAE(CAPS, TAP) / SAE(NEPH), as a function of 630nm wavelength SSA(NEPH, CAPS) values for AQ/AS mixtures. The 630 nm wavelength light absorption coefficient, σ_{ap}(TAP), is used as the colour code.

~~When comparing the SAE dataset obtained by using Nephelometer and CAPS is measurements in Figure 12 and Table 12, Aquadag shows the best instrument-to-instrument ratio of 0.99 + 0.15. A small nonlinearity for SAE values higher 3.0 begins to deviate from the 1:1 line but stays within 15% deviation, as already seen for EAE. Here, again, NEPH shows higher SAE values compared to CAPS by a factor 0.9. This factor corresponds as with the observed factor for the EAE values and is linked to nephelometer measurements for fine AS particles. Since the Nephelometer correction is calculated based on the scattering angstrom exponent, which contains a vague size distribution information, it could fail to give correct values for aerosol mixtures and for different sizes.~~

3~~2~~.3~~2~~.5 Absorbing~~4~~ Ångström exponent (~~:~~ AAE)

The absorption Ångström exponent (AAE) depends entirely on the absorbing particle type and coatings and should not differ when the light absorbing particles ~~is~~ are externally mixed with non-light absorbing particles. Thus, scatter plots of AAE values should exhibit a single point. Figure 13 shows the derived AAE(CAPS, NEPH) values relative to the derived AAE(TAP) values for pure AQ and for AQ/AS external mixtures. The AAE(TAP) values were chosen as the reference measurements here, despite the potential for known filter-based artifacts. The pure AQ measurements in Figure 13 exhibit a compact cluster around AAE ~ 0.4, indicating a well-defined (i.e., small variance) set of AAE measurements were obtained for both AAE measurements. The measured AAE for pure AQ particles of 0.4 is consistent with the "close to zero" result reported by ~~(~~Aiken., ~~(~~2016 ~~#294) Aiken et al. (2016~~).

The externally mixed AQ/AS results show a significantly different result. For the AQ/AS mixtures, the AAE(TAP) exhibited a similar variance as for the pure AQ aerosols, while the AAE(CAPS, NEPH) values exhibited a much larger variance, including unphysical negative values. One reason for the larger AAE(CAPS, NEPH) variances observed for the externally AQ/AS mixtures relative to the pure AQ is that the mixed AQ/AQ samples were conducted at significantly lower AQ loadings (i.e., lower σ_{ap} values). Another reason is that the pure AQ aerosols exhibited the lowest SSA values (~0.37 from Table 3) relative to the AQ/AS external mixtures.

Figure 14 shows the ratio AAE(CAPS, NEPH) / AAE(TAP) versus the 630 nm wavelength SSA(NEPH, CAPS) values. As predicted in the propagated error analysis shown in Figure 6, higher SSA values cause higher uncertainties in Differential Method calculated light absorption coefficients, σ_{ap}(DM), and, therefore, the derived AAE(CAPS, NEPH) values. In fact, since the derived AAE(CAPS, NEPH) values depend upon σ_{ap}(DM) measurements at two different wavelengths, the AAE uncertainties will be significantly higher than the corresponding σ_{ap}(DM) uncertainties, especially at high SSA values. Figure 14 indicates that lowering the absorption coefficients below 50 Mm^{-1} or increasing the SSA above 0.5, the derived AAE(CAPS, NEPH) values begin to vary strongly relative to the

AAE(TAP) values. For laboratory studies, aerosols with similar low SSA values and high absorbing particle concentrations can be readily achieved, but are rarely present in the ambient atmosphere. Therefore, extreme caution is justified when attempting to derive ~~EAE~~AAE(CAPS, NEPH) values for atmospheric measurements.

~~The particles are external mixtures. Two separate nebulizers were used, as well as two separate dryer tubes. After that they are mixed in a chamber. Thus, the AAE for all mixtures should depend only on the absorbing aerosol distributions and be independent of the non-absorbing particles. This independency of adding AS to the mixture was observed for the filter based instrument TAP, visible as x-axes in the scatter plot Figure 13, but when the AAE was calculated using measurements of the in-situ instruments Nephelometer and CAPS, the AAE deviates more with increasing SSA and lowering σ_{ap} shown in Figure 14. For mixtures of AQ, the AAE (CAPS, NEPH) is calculated~~could reach ~~even unphysical negative values. As a result of the error propagation for precision errors, shown as individual error bars in both figures, it can be stated that AAE(CAPS,NEPH) values are not trustworthy especially for AQ mixtures with AAE(TAP) < 1.~~

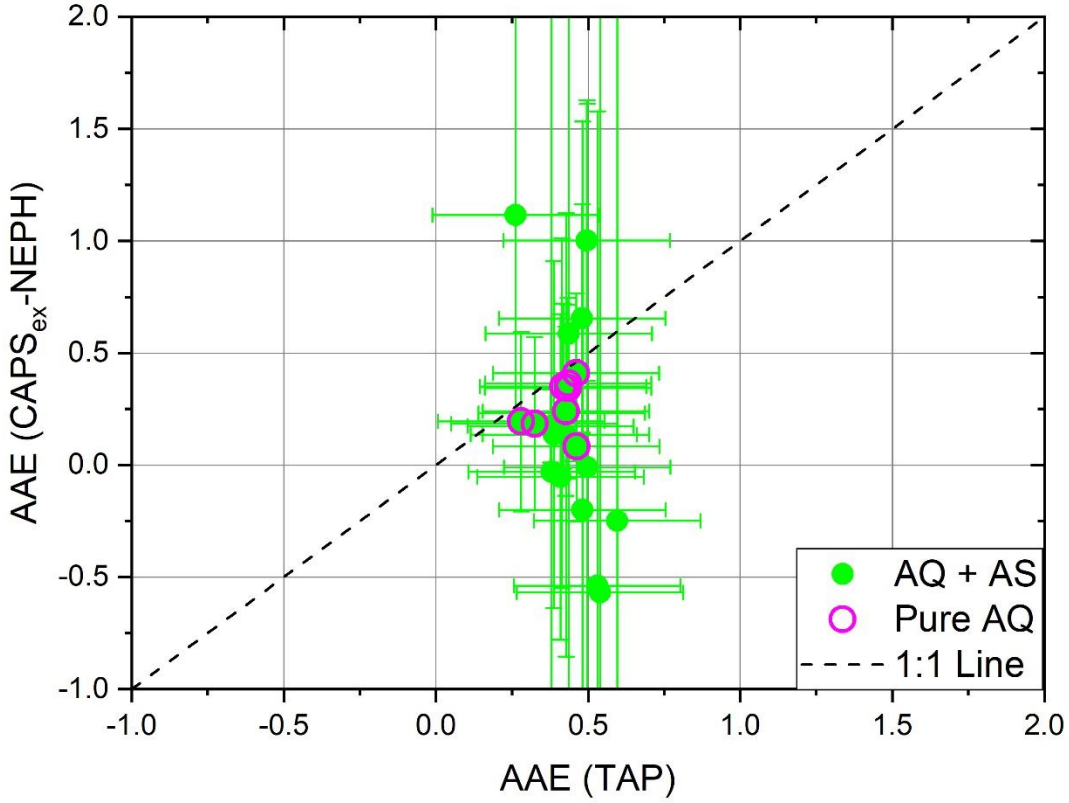
AAE (CAPS$_{ex}$-NEPH)
AAE (TAP)
2.0
1.5
1.0
0.5
0.0
-0.5
-1.0
-1.0
-0.5
0.0
0.5
1.0
1.5
2.0
AQ + AS
Pure AQ
1:1 Line

950

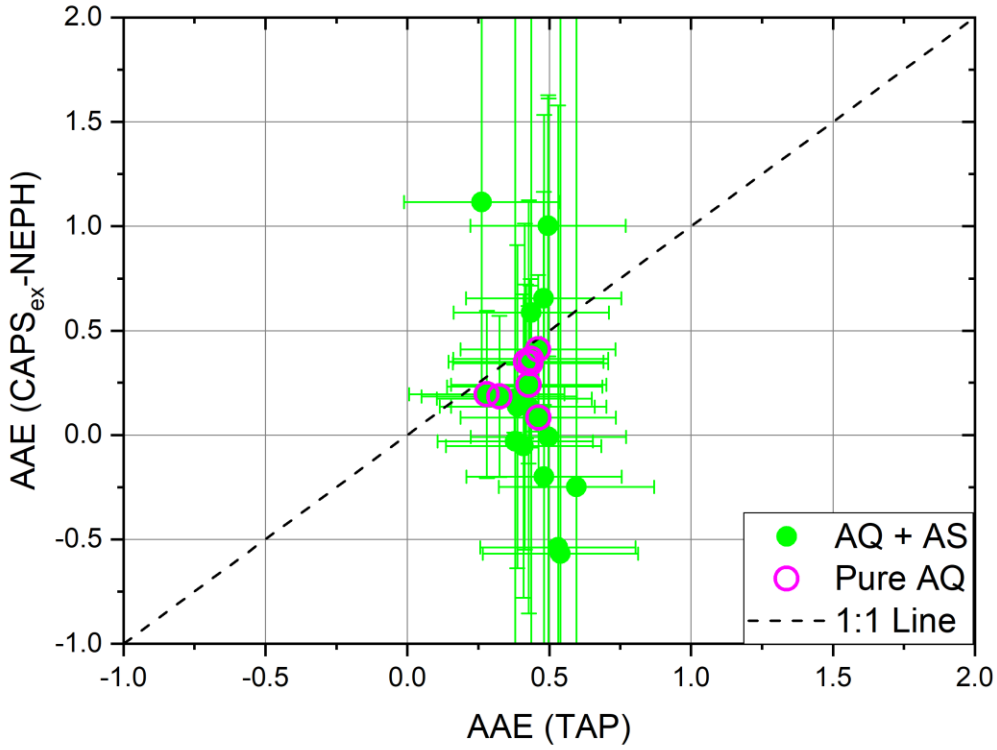

Figure 11~~13~~. Scatter plot of AAE(CAPS, NEPH) measurements compared to AAE(TAP) measurements for pure AQ and AQ/AS external mixtures. Measured precision error bars are shown for individual AQ/AS externally mixed measurements.~~**Scatter plot of AAE values obtained by AAE(TAP) compared to AAE(CAPS, NEPH).**~~

~~The reason for this is the high relative precision error associated with low absorption particle loads for AAE (CAPS, NEPH), which we had crosschecked by calculating the variation of the AAE by varying the input variables by their possible max errors, showing the same results. Pure Aquadag particles are made visible by an open circle and it is visible, that those does not stray far from the 1:1 line in Figure 13 including AAE vales for Aquadag. For the pure substance a higher particle load could be used and no other negative interfering non absorbing aerosols influence the measurements.~~

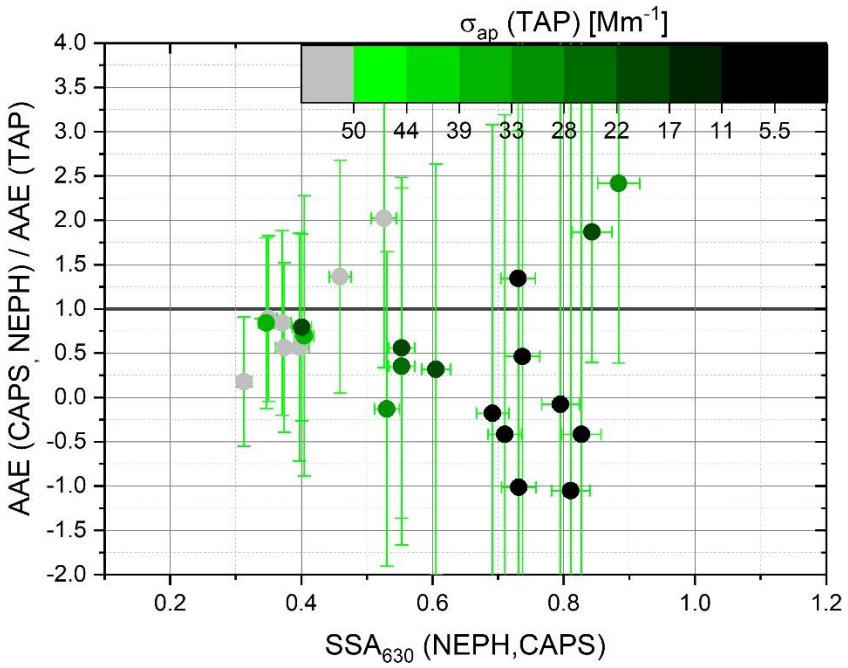

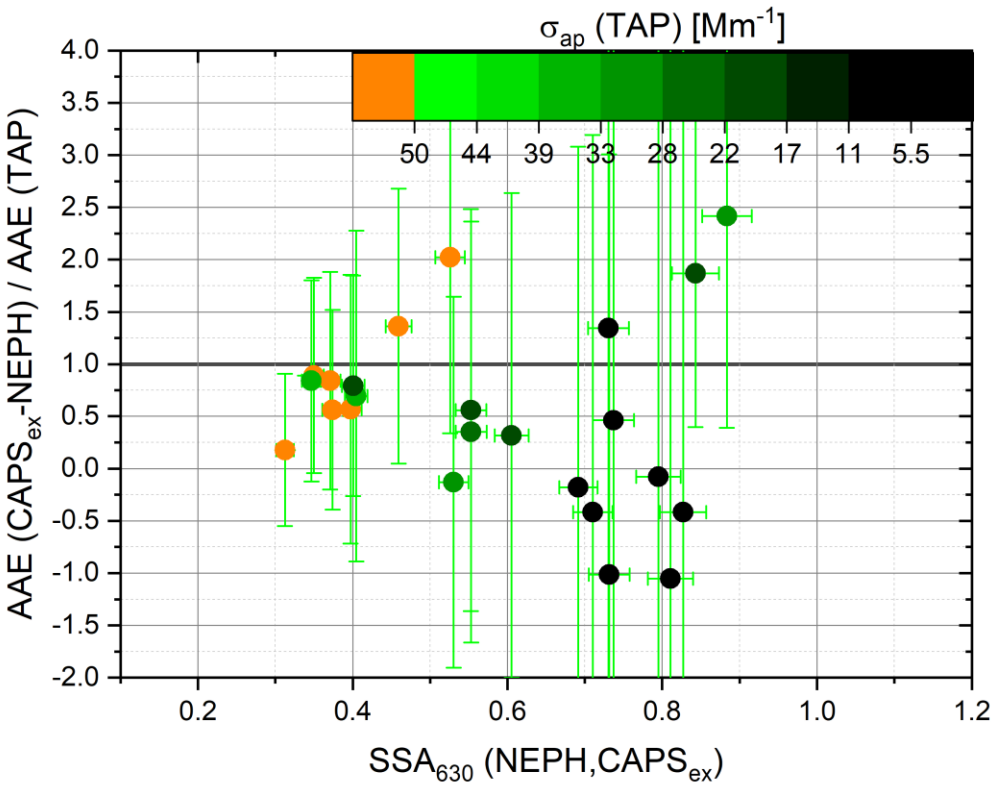

Figure 12~~14~~. The absorbing Ångström exponent ratio, AAE(CAPS, NEPH) / AAE(TAP), as a function of 630 nm wavelength SSA(NEPH, CAPS) values for AQ/AS mixtures. The 630 nm wavelength light absorption coefficient,

σ_{ap}(TAP), is used as the colour code. Measured precision error bars are shown for individual measurements. ~~This figure shows the instrument to instrument ratio of the absorption Ångström exponent AAE(CAPS, NEPH) / AEAE(TAP) are shown as functions of SSA(CAPS, NEPH) 630nm and information of light absorption coefficient σ_{ap}(TAP) as a colour code are shown.~~

~~In Figure 14, showing the Method-to-method ratios AAE(CAPS, NEPH) / AEAE (TAP) there is a strong dependency as function ofon σ_{ap}(TAP) and SSA(CAPS,NEPH)_630 visible. Lowering the absorption coefficients below 100 Mm^{-1} or a SSA higher than 0.5, the AAE begins to differ strongly and up to tends up to triple the AAE value calculated from TAP coefficients only. As long as forFor laboratory studies, these high particle concentrations could be archived, but are rarely present in atmospheric conditions EAE(CAPS, NEPH) method is not applicable for atmospheric measurements~~

Table 12 summarizes the averages and standard deviations of the measured Ångström exponent ratios, EAE(NEPH, TAP) / EAE(CAPS), SAE(CAPS, TAP) / SAE(NEPH), and AAE(CAPS, NEPH) / AAE(TAP). The average Ångström exponent ratios for light extinction (EAE) and scattering (SAE) fall within 10% of unity, with SOOT exhibiting the large variances. The average Ångström exponent ratios for light absorption (AAE) exhibit large deviations from unity with even larger variances. A large deviation for the AAE ratios value is associated with weak absorption coefficients of the aerosol mixtures used. Therefore, the AAE values show the biggest differences within the instrument-to-instrument ratio analysis.

Table 1~~1~~2~~2~~. Ensemble averages and standard deviations for the instrument-to-instrument ratios of the Ångström exponents (EAE, SAE, AAE) derived from multiple instruments relative to those derived from single instruments as reference. ~~using Ångström exponent calculated using instrument calculations and Ångström exponents (EAE, SAE, AAE) using single instrument data as reference.~~

Ångström coefficient ratio	BC	AQ	SOOT	MB
EAE(~~Neph~~NEPH, TAP) / EAE(CAPS)	0.92 ± 0.07	1.05 ± 0.15	0.99 ± 0.56	0.97 ± 0.15
SAE(CAPS, TAP) / SAE(~~Neph~~NEPH)	1.13 ± 0.10	0.99 ± 0.15	1.43 ± 0.61	1.09 ± 0.15
AAE(CAPS, NEPH) / AAE(TAP)	1.72 ± 0.85	0.39 ± 1.70	1.19 ± 0.93	0.91 ± 2.32

~~To compare the overall accuracy of the instrument to instrument rations are compiled~~ results ~~for EAE(NEPH,TAP)/EAE(CAPS), SAE(CAPS,TAP)/SAE(NEPH) and AAE(CAPS,NEPH)/AEA(TAP) are shown in Table 12. Here, an ensemble average and the associated variance was considered as a good reference. The instrument to instrument ratios for Ångström exponents for light extinction and Ångström exponents for scattering correspond within 10% deviation. The most prominent exception~~exception is , ~~is again~~ , ~~freshly produced combustion soot. For light absorption, a large deviation for the AAE ratios value is associated with weak absorption coefficients of the mixtures used. Therefore, the AAE shows the biggest differences within the instrument to instrument ratio analysis.~~

~~4~~3. Conclusions

A major goal of this study was to determine if the ~~the errors associated with instrumental uncertainties of~~ intensive optical aerosol parameters, ~~such as~~ single scattering albedo and Ångström exponents, for externally mixed absorbing and non-absorbing aerosols could be measured within reported optical instrument extensive measurement uncertainties (i.e., optical closure). Closure within reported instrument uncertainties was achieved for all measured extensive optical properties (i.e., extinction, scattering, and absorption) and most intensive optical properties (i.e., single scattering albedo, extinction Ångström exponent and scattering Ångström exponent). Unsurprisingly, the measurements with the largest variances were the absorption coefficient measurements derived from the Differential Method (i.e., absorption = extinction minus scattering) and the related absorbing Ångström exponent (AAE). While the absorption coefficient measurements were within reported uncertainties, the derived AAE values exhibited average values and standard deviations ~~greater than expected~~far greater than the other Ångström exponent but are within expected range.

We conducted an~~Basis was an~~ instrument intercomparison laboratory study ~~of~~ employing several widely used measurement techniques ~~that are~~ suitable for long-term ambient observations. The optical instrument suite included two CAPS PM_{SSA} monitors measuring extinction and scattering at 450 and 630nm, a TSI integrating Nephelometer (NEPH) measuring scattering at 450, 550, and 700 nm, and a Brechtel Tricolor Absorption Photometer (TAP) measuring absorption at 467, 528, and 652 nm. External mixtures of absorbing (Aquadag, combustion soot from a laboratory flame generator, Cabot carbon black, and acrylic Magic Black paint) particles and non-absorbing ammonium sulphate particles were generated with single scattering albedo (SSA) values between 0.2 and 1.0 and extinction values between 15 – 150 Mm^{-1}, representative of atmospheric aerosols. However, our study does not explicitly address real-world ambient aerosols that can be internally or externally mixed or both, contain particles with liquid, solid, and/or semi-solid phases, and may contain multiple sources of absorbing material.

~~The methods used agreed the most for~~ with ~~a mixture of the spherical shaped colloidal graphite (Aquadag) as light absorbing and ammonium sulphate as~~ a ~~light scattering aerosol component. Results for this mixture have low uncertainties and agree within 10% deviation between the methods for single scattering albedo, extinction Ångström exponent and scattering Ångström exponent. Laj et al.,2020 recently stated requirements for GCOS (Global Climate~~

~~Observing System) applications. Here, he proposed uncertainties lower than the 20% measurement uncertainty for single scattering albedo measurements for attributing and detecting changes to a climate feedback. The uncertainties and deviations shown in this work are with 8-10% measurement uncertainty fulfil the required limit.~~ Overall, we were able to show ~~study~~ that measured extensive optical parameters agree within the limits of uncertainty for the individual or combined instruments. In particular, we report that the scattering coefficient measurement by the CAPS PM_{SSA} agrees with the TSI integrating Nephelometer within 10% relative error (i.e., optical closure). Therefore, The CAPS PM_{SSA} monitor could be considered as a replacement for the TSI Nephelometer, as the NEPH is no longer produced. Trade-offs in the CAPS PM_{SSA} versus NEPH comparison include the three wavelengths and backscatter measurements of the NEPH versus the single wavelength of the CAPS PM_{SSA}, countered by the additional extinction measurement of the CAPS PM_{SSA} allowing for absorption and SSA values to be simultaneously measured.

Measurement differences were observed as a function of absorbing particle type. For light absorbing compact aggregates, we achieved the highest correlations for light extinction, scattering, and absorption coefficients. For fractal-like absorbing combustion soot particles, the correlation for light absorption between the in-situ and filter methods weakened but stayed within instrument uncertainty ranges. These observed differences might be due to the combined effects of small flickers from the inverted flame generator during the experiment, the overall filter correction schemes, and/or the physical behaviour of agglomerates. For more compact particles, the scattering is stronger (Radney et al., 2014). For the TAP filtered-based method, changes in the backscattering of light is not considered in the correction schemes, which might be responsible for the disagreement.

~~For compact aggregatesspherical particles, we achieved the highest correlations for each light extinction, scattering and absorption coefficients. For fractal-like particles, the correlation for light absorption between the in-situ and filter method weakens but stays within instrument uncertainty ranges.~~

Uncertainties increased for intensive optical parameters, especially for the absorption Ångström exponent (AAE) parameter that relied ons ~~obtained with~~ the differential method ~~that calculates~~to calculate light absorption as the difference between light extinction and light scattering. The intensive parameters for the scattering and extinction Ångström exponent were within 10% relative error (i.e., optical closure), regardless of which instrument combination was used for parameter derivation. In contrast, absorption Ångström exponent (AAE) values required~~In addition, extinction Ångström exponents, scattering Ångström exponents, and single scattering albedo were not as much affected by the uncertainties associated with the differential method used for σ_{ap} compared to the absorption Ångström exponent. Using the differential method, AAE was rarely within typical physical values for the differential method.~~ L low ~~single scattering albedo~~SSA values (<0.5) and~~,~~ ~~more importantly,~~ high ~~particle loads of~~particulate absorption values ~~at least~~(>~~50 Mm^{-1}~~) ~~are~~were necessary to reach satisfactory levels of measurement uncertainty ~~levels. for the DM Low single scattering albedo values (<0.5) and, more importantly, high particle loads of at least 50 Mm^{-1} are necessary to reach satisfactory uncertainty levels~~. Similar AAE results were recently reported for rural background sampling (Asmi et al., 2021).

Even with the strong deviation within absorption values, the intensive parameters for the scattering and extinction Ångström exponent stay within 10% deviation, regardless of which instrument combination is used for calculation. With this approach the intensive aerosol properties showed a high rate of agreement between different instrument sets for the determination of these properties for techniques used for long-term measurements, except for the absorption angstrom exponent.

It was recently shown, that for rural areas these values are not achievable and show high deviations for detection limits and environmental monitoring for DM and filter based measurements ({Asmi et al., 2021}). Additionally, our study does not explicitly address real-world ambient aerosols that can be internally or externally mixed or both, contain particles with liquid, solid, and semi-solid phases, and may contain multiple sources of absorbing material1 #289}. It was shown in {Lack, 2008, that environmental measurements could be troublesome with filter methods, but we are most certain, that for intensive Parameter calculation these values could still be used. #18} In our study, Ffreshly-generated combustion soot differs the most, with results disagreeing up to 30% between filter based absorption coefficient data and in situ methods. This is due to the combined effects of small flickers of the inverted flame generator during the experiment, the overall filter correction schemes, and the physical behaviour of agglomerates. For more compact particles, the scattering is stronger ({Radney et al., 2014 #291}). A stronger backscattering is not considered in the correction schemes which might be responsible for the disagreement. The single scattering albedo for 630 nm wavelength could be determined within 10% deviation between the instrument combinations of CAPS, TAP and Integrating Nephelometer, but tends to differ by at least 0.1 for light absorption coefficients of over 50 Mm^{-1}. A similar accuracy could be achieved with a wavelength of 450 nm, for which a 15% deviation between the instrument combinations must be considered. Even with the strong deviation within absorption values, the intensive parameters for the scattering and extinction Ångström exponent stay within 10% deviation, regardless of which instrument combination is used for calculation. With this approach the intensive aerosol properties showed a high rate of agreement between different instrument sets for the determination of these properties for techniques used for long-term measurements, except for the absorption angstrom exponent. As an additional result, we can present that in our study, the scattering coefficient measurement by the CAPS PM_{SSA} agrees with the integrating Nephelometer within 10% deviation. Therefore, it could be substituting the TSI Nephelometer 3563 for light scattering measurements since it is not produced any longer.

This does not mean that nephelometer are not of interest anymore because the provide additional information on backscattering information at multiple wavelength in one instrument.As an additional result, we can present that for stable aerosol production, the internal scattering coefficient measurement by the CAPS PM_{SSA} agrees with the integrating Nephelometer within 10% deviation and therefore could be substitute the TSI Nephelometer 3563 for light scattering measurements which is not produced any longer.

Finally, Laj et al. (2020) recently stated measurement requirements for GCOS (Global Climate Observing System) applications for attributing and detecting changes to climate feedback. The reported requirements for the climate-critical intensive optical properties, specifically the single scattering albedo (SSA), are measurement techniques with relative measurement uncertainties less than 20%. In our study, SSA values were measured for all instrument combinations of CAPS, TAP, and NEPH within 10% relative error at 630 nm wavelength and within 15% at 450 nm

wavelength. Therefore, the measured SSA averages and variances using our optical instrument suite for externally mixed laboratory particles indicates that these instruments meet these proposed requirements.

Acknowledgments. Parts of this work were supported by IAGOS-D (Grant Agreement No. 01LK1301A), EU H2020 Project ENVRIplus (Grant No.654182) and HITEC Graduate School for Energy and Climate. A special thanks to Paola Formenti for her assistance with the manuscript.

Contributions of co-authors. PW performed all instrument calibrations, the instrumental set up, and the data analysis. UB and BF designed the LabVIEW environment of the experimental set up. MB helped during instrument preparations. AF and TO provided technical details of the instrumentation. PW, OB,, AF, TO, UB and AP contributed to the manuscript and the interpretation of the results.

Conflict of interest. The authors declare that they have no conflict of interest.

~~Data availability.~~

References

Anderson, T. L. and Ogren, J. A.: Determining aerosol radiative properties using the TSI 3563 integrating nephelometer, Aerosol Science and Technology, 29, 57-69, 1998.

Ångström, A.: On the Atmospheric Transmission of Sun Radiation and on Dust in the Air, Geografiska Annaler, 11, 156-166, 1929.

Barber, P. W. and Wang, D.-S.: Rayleigh-Gans-Debye applicability to scattering by nonspherical particles, Appl. Opt., 17, 797-803, 1978.

Bischof, O., Weber, P., Bundke, U., Petzold, A., and Kiendler-Scharr, A.: Characterization of the Miniaturized Inverted Flame Burner as a Combustion Source to Generate a Nanoparticle Calibration Aerosol, doi: 10.1007/s40825-019-00147-, 2019. 1-10, 2019.

Bodhaine, B. A., Ahlquist, N. C., and Schnell, R. C.: Three-wavelength nephelometer suitable for aircraft measurement of background aerosol scattering coefficient, Atmospheric Environment. Part A. General Topics, 25, 2267-2276, 1991.

Bohren, C. F. and Huffman, D. R.: Absorption and scattering of light by small particles, 1983.

Bond, T. C., Anderson, T. L., and Campbell, D.: Calibration and intercomparison of filter-based measurements of visible light absorption by aerosols, Aerosol Science and Technology, 30, 582-600, 1999.

Collaud Coen, M., Weingartner, E., Apituley, A., Ceburnis, D., Fierz-Schmidhauser, R., Flentje, H., Henzing, J. S., Jennings, S. G., Moerman, M., Petzold, A., Schmid, O., and Baltensperger, U.: Minimizing light absorption measurement artifacts of the Aethalometer: evaluation of five correction algorithms, Atmos. Meas. Tech., 3, 457-474, 2010.

Faria, J., Bundke, U., Freedman, A., Onasch, T., and Petzold, A.: Laboratory Validation and Field Deployment of a Compact Single-Scattering Albedo (SSA) Monitor, Atmospheric Measurement Techniques Discussions, doi: 10.5194/amt-2019-146, 2019. 1-18, 2019.

Formenti, P., Schütz, L., Balkanski, Y., Desboeufs, K., Ebert, M., Kandler, K., Petzold, A., Scheuvens, D., Weinbruch, S., and Zhang, D.: Recent progress in understanding physical and chemical properties of African and Asian mineral dust, Atmos. Chem. Phys., 11, 8231-8256, 2011.

Foster, K., Pokhrel, R., Burkhart, M., and Murphy, S.: A novel approach to calibrating a photoacoustic absorption spectrometer using polydisperse absorbing aerosol, Atmos. Meas. Tech., 12, 3351-3363, 2019.

Hansen, A. D. A., Rosen, H., and Novakov, T.: The aethalometer — An instrument for the real-time measurement of optical absorption by aerosol particles, Science of The Total Environment, 36, 191-196, 1984.

Kaskaoutis, D. G., Kambezidis, H. D., Hatzianastassiou, N., Kosmopoulos, P. G., and Badarinath, K. V. S.: Aerosol climatology: on the discrimination of aerosol types over four AERONET sites, Atmos. Chem. Phys. Discuss., 2007, 6357-6411, 2007.

Kazemimanesh, M., Moallemi, A., Thomson, K., Smallwood, G., Lobo, P., and Olfert, J.: A novel miniature inverted-flame burner for the generation of soot nanoparticles, Aerosol Science and Technology, doi: 10.1080/02786826.2018.1556774, 2018. 2018.

Kim, J., Bauer, H., Dobovičnik, T., Hitzenberger, R., Lottin, D., Ferry, D., and Petzold, A.: Assessing Optical Properties and Refractive Index of Combustion Aerosol Particles Through Combined Experimental and Modeling Studies, Aerosol Science and Technology, 49, 340-350, 2015.

Kirchstetter, T. W. and Thatcher, T. L.: Contribution of organic carbon to wood smoke particulate matter absorption of solar radiation, Atmos. Chem. Phys., 12, 6067-6072, 2012.

Kokhanovsky, A.: Aerosol Optics: Light Absorption and Scattering by Particles in the Atmosphere, 2008.

Massoli, P., Murphy, D. M., Lack, D. A., Baynard, T., Brock, C. A., and Lovejoy, E. R.: Uncertainty in Light Scattering Measurements by TSI Nephelometer: Results from Laboratory Studies and Implications for Ambient Measurements, Aerosol Science and Technology, 42, 1064-1074, 2009.

Modini, R. L., Corbin, J. C., Brem, B. T., Irwin, M., Bertò, M., Pileci, R. E., Fetfatzis, P., Eleftheriadis, K., Henzing, B., Moerman, M. M., Liu, F., Müller, T., and Gysel-Beer, M.: Detailed characterization of the CAPS single-scattering albedo monitor (CAPS PMssa) as a field-deployable instrument for measuring aerosol light absorption with the extinction-minus-scattering method, Atmos. Meas. Tech., 14, 819-851, 2021.

Moosmüller, H., Chakrabarty, R. K., and Arnott, W. P.: Aerosol light absorption and its measurement: A review, Journal of Quantitative Spectroscopy and Radiative Transfer, 110, 844-878, 2009.

Müller, T., Virkkula, A., and Ogren, J. A.: Constrained two-stream algorithm for calculating aerosol light absorption coefficient from the Particle Soot Absorption Photometer, Atmos. Meas. Tech., 7, 4049-4070, 2014.

Myhre, G., Shindell, D., Bréon, F.-M., Collins, W., Fuglestvedt, J., Huang, J., Koch, D., Lamarque, J.-F., Lee, D., Mendoza, B., Nakajima, T., Robock, A., Stephens, G., Takemura, T., and Zhang, H.: Anthropogenic and Natural Radiative Forcing. In: Climate Change 2013: The Physical Science Basis. Contribution of Working Group I to the Fifth Assessment Report of the Intergovernmental Panel on Climate Change, Stocker, T. F., Qin, D., Plattner, G.-K., Tignor, M., Allen, S. K., Boschung, J., Nauels, A., Xia, Y., Bex, V., and Midgley, P. M. (Eds.), Cambridge University Press, Cambridge, United Kingdom and New York, NY, USA, 2013.

Ogren, J., Wendell, J., Andrews, E., and Sheridan, P.: Continuous light absorption photometer for long-Term studies, Atmospheric Measurement Techniques, 10, 4805-4818, 2017.

Onasch, T., Massoli, P., Kebabian, P., Hills, F. B., Bacon, F., and Freedman, A.: Single Scattering Albedo Monitor for Airborne Particulates, Aerosol Science and Technology, 49, 267 - 279, 2015.

Petzold, A., Ogren, J. A., Fiebig, M., Laj, P., Li, S. M., Baltensperger, U., Holzer-Popp, T., Kinne, S., Pappalardo, G., Sugimoto, N., Wehrli, C., Wiedensohler, A., and Zhang, X. Y.: Recommendations for reporting "black carbon" measurements, Atmos. Chem. Phys., 13, 8365-8379, 2013.

Petzold, A., Rasp, K., Weinzierl, B., Esselborn, M., Hamburger, T., DöRnbrack, A., Kandler, K., SchuüTz, L., Knippertz, P., Fiebig, M., and Virkkula, A.: Saharan dust absorption and refractive index from aircraft-based observations during SAMUM 2006, Tellus B: Chemical and Physical Meteorology, 61, 118-130, 2009.

Petzold, A., Schloesser, H., Sheridan, P., Arnott, W., Ogren, J., and Virkkula, A.: Evaluation of Multiangle Absorption Photometry for Measuring Aerosol Light Absorption, Aerosol Science and Technology, 39, 40-51, 2005.

Rosen, H., Hansen, A. D. A., Gundel, L., and Novakov, T.: Identification of the optically absorbing component in urban aerosols, Appl. Opt., 17, 3859-3861, 1978.

Russell, P. B., Bergstrom, R. W., Shinozuka, Y., Clarke, A. D., DeCarlo, P. F., Jimenez, J. L., Livingston, J. M., Redemann, J., Dubovik, O., and Strawa, A.: Absorption Angstrom Exponent in AERONET and related data as an indicator of aerosol composition, Atmos. Chem. Phys., 10, 1155-1169, 2010.

Sandradewi, J., Prévôt, A. S. H., Szidat, S., Perron, N., Alfarra, M. R., Lanz, V. A., Weingartner, E., and Baltensperger, U.: Using Aerosol Light Absorption Measurements for the Quantitative Determination of Wood Burning and Traffic Emission Contributions to Particulate Matter, Environmental Science & Technology, 42, 3316-3323, 2008.

Schnaiter, M., Schmid, O., Petzold, A., Fritzsche, L., Klein, K. F., Andreae, M. O., Helas, G., Thielmann, A., Gimmler, M., Mohler, O., Linke, C., and Schurath, U.: Measurement of wavelength-resolved light absorption by aerosols utilizing a UV-VIS extinction cell, Aerosol Science and Technology, 39, 249-260, 2005.

Sheridan, P. J., Arnott, W. P., Ogren, J. A., Andrews, E., Atkinson, D. B., Covert, D. S., Moosmüller, H., Petzold, A., Schmid, B., Strawa, A. W., Varma, R., and Virkkula, A.: The Reno Aerosol Optics Study: An Evaluation of Aerosol Absorption Measurement Methods, Aerosol Science and Technology, 39, 1-16, 2005.

Veselovskii, I., Goloub, P., Podvin, T., Bovchaliuk, V., Derimian, Y., Augustin, P., Fourmentin, M., Tanre, D., Korenskiy, M., Whiteman, D. N., Diallo, A., Ndiaye, T., Kolgotin, A., and Dubovik, O.: Retrieval of optical and physical properties of African dust from multiwavelength Raman lidar measurements during the SHADOW campaign in Senegal, Atmos. Chem. Phys., 16, 7013-7028, 2016.

Virkkula, A.: Correction of the Calibration of the 3-wavelength Particle Soot Absorption Photometer (3 PSAP), Aerosol Science and Technology, 44, 706-712, 2010.

Xu, L., Suresh, S., Guo, H., Weber, R. J., and Ng, N. L.: Aerosol characterization over the southeastern United States using high-resolution aerosol mass spectrometry: spatial and seasonal variation of aerosol composition and sources with a focus on organic nitrates, Atmos. Chem. Phys., 15, 7307-7336, 2015.